Directions for Use of Density Functional Theory: A Short Instruction Manual for Chemists

6

Heiko Jacobsen and Luigi Cavallo

Contents

H. Jacobsen (✉)
KemKom, New Orleans, LA, USA
e-mail: jacobsen@kemkom.com

L. Cavallo
Physical Sciences and Engineering Division, Kaust Catalysis Center, King Abdullah University of Science and Technology (Kaust), Thuwal, Saudi Arabia
e-mail: Luigi.Cavallo@kaust.edu.sa

J. Leszczynski et al. (eds.), *Handbook of Computational Chemistry*,
DOI 10.1007/978-3-319-27282-5_4

Abstract

Two aspects are quintessential if one seeks to successfully perform DFT calculations: a basic understanding of how the concepts and models underlying the various manifestations of DFT are built and an essential knowledge of what can be expected from DFT calculations and how to achieve the most appropriate results. This chapter expands on the development and philosophy of DFT and aims to illustrate the essentials of DFT in a manner that is intuitively accessible. An analysis of the performance and applicability of DFT focuses on a representative selection of chemical properties, including bond lengths, bond angles, vibrational frequencies, electron affinities and ionization potentials, atomization energies, heats of formation, energy barriers, bond energies, hydrogen bonding, weak interactions, spin states, and excited states.

Introduction

Density functional theory (DFT) is an enticing subject. It appeals to chemists and physicists alike, and it is entrancing for those who like to work on mathematical physical aspects of problems, for those who relish computing observable properties from theory, and for those who most enjoy developing correct qualitative descriptions of phenomena. It is this combination of a qualitative model that at the same time furnishes quantitative reliable estimates that makes DFT particularly attractive for chemists.

DFT is an alternative, and complementary, to wave function theory (WFT). Both approaches are variations of the basic theme of electronic structure theory, and both methods originated during the late years of the 1920s. Whereas WFT evolved rapidly and gained general popularity, DFT found itself in a state of shadowy existence. It was the appearance of the key papers by Hohenberg and Kohn (1964) and by Kohn and Sham (1965), generally perceived as the beginning of modern DFT, which changed the perception and level of acceptance of DFT. With the evolution of reliable computational technologies for DFT chemistry, and with the advent of the generalized gradient approximation (GGA) during the 1980s, DFT emerged as powerful tool in computational chemistry, and without exaggeration the 1990s can be called the decade of DFT in electronic structure theory. During this time period, despite the lack of a complete development, DFT was already competitive with the best WFT methods. Furthermore, the advancement of computational hardware as well as software has progressed to a state where DFT calculations of "real molecules" can be performed with high efficiency and without major technical hurdles.

But at the end of the first decade of the new millennium, it appeared that DFT might have become a victim of its own success. DFT has transformed into an off-the-shelf technology and ready-to-crunch component and often was and still is used as such. Still and all, it became clear that the happy days of black-box DFT were over and that not all the promises of DFT came to fruition. DFT has its

own limitations and shortcomings, and the numbers obtained from DFT calculations began to lose some of their awe-inspiring admiration they enjoyed at the end of the first millennium. At the same time, DFT has matured into a standard research tool, used routinely by many experimental chemists to support their work.

Despite the fact that DFT has evolved into a first-choice approach for a stunning potpourri of applications throughout chemistry and materials science, it is all too well known that DFT in its current form still has serious limitations; Cohen et al. (2012) identify and analyze current challenges to DFT. Moreover, it appears that the philosophical, theoretical, and computational framework of DFT might lose its prominent position in electronic structure theory. Fifty years after its formal inception, Becke (2014) reviewed the development and current status of Kohn–Sham density functional theory and raises the concern that increasing pressure to deliver higher and higher accuracy and to adapt to ever more challenging problems "may submerge the theory in the wave-function sea" (Becke 2014). But in whatever direction the path of extended development will guide users and developers of DFT, it seems evident that DFT will continue its role as research tool not only for computational but also for theoretical inclined chemists.

We have composed our short instruction manual for chemists in view of the ontogeny of DFT. A chemist using DFT calculations should be aware of the fact that all approximations and simplifications of any general theory may lead to failures in computed data. Every principally correct theory, if not executed with specific care, may produce essentially wrong results and therefore erroneous predictions. Two aspects are quintessential if one seeks to successfully perform DFT calculations: a basic understanding of how the concepts and models underlying the various manifestations of DFT are built and an essential knowledge of what can be expected from DFT calculations and how to achieve the most appropriate results. Thus, we have divided the main body of our directions into two parts.

In section "DFT: A Paradigm Shift in Theoretical Chemistry," we expand on the development and philosophy of DFT. We do not present a course or textbook work on DFT; the interested reader will find a selection of references to the literature for more elaborate and detailed descriptions. Rather, we aim to illustrate the essentials of DFT in a manner that is intuitively accessible. For this reason, we will avoid mathematical equations as much as possible, incorporate formulas into the flow of the text, and only on occasion add the odd-numbered equation to the elaboration. As a consequence, we have to abandon the rigor that unambiguous and well-defined derivations require and introduce a certain degree of sloppiness. We hope that such a treatment will facilitate the flow of our arguments and emphasize that what we think are indispensable aspects of DFT.

In section "DFT: Computational Chemistry in Action," we present an analysis of the performance and applicability of DFT. We focus on a representative selection of chemical properties and system types and base our review on a selection of representing benchmarking studies, which encompass several well-established density functionals together with the most recent efforts in the field. Due to the multitude of papers that report DFT applications, our analysis is far from complete,

but we aim to present a representative snapshot of the current situation of DFT at the beginning of the second decade of the new millennium.

We will close our work with two additional short sections "DFTips" and "A Concise Guide to the Literature," where we present the reader with a few tips how to use DFT, and with a collection of selected references as a concise guide to the by now vast literature of DFT.

DFT: A Paradigm Shift in Theoretical Chemistry

Density functional theory is primarily a theory of electronic ground-state structure, which is based on the electron density distribution $\rho(r)$. In contrast to DFT, wave function theory is an approach to electronic structure, which is based on the many-electron wave function $\Psi(\mathrm{r}_n)$. In order to put the innovation of DFT into proper perspective, we begin with a brief overview of WFT, before we illustrate the essentials and growth of DFT.

The objective of WFT is the exact solution of the time-independent Schrödinger equation (TISE), $\mathrm{H}\Psi = E\Psi$, for a system of interest. [We recall that in quantum mechanics, associated with each measurable parameter in a physical system is an operator, and the operator associated with the energy of a system is called the Hamiltonian H. The Hamiltonian contains the operations associated with the kinetic and potential energies of all particles that comprise a system. We further note that the terms function, operator, and functional are to be understood such that a function is a prescription which maps one or more numbers to another number, an operator is a prescription which maps one function to another function, and a functional takes a function and provides a number.] The solution to the TISE yields the wave function Ψ as well as the energy E for the system of interest. In a systematic, variational search, one looks for the wave function that produces the lowest energy and arrives at a description for the system in its ground state.

If we consider a system of nuclei and N electrons, solving the TISE – within the Born–Oppenheimer separation between the apathetic ambulation of nuclei and the rapid ramble of electrons – yields the electronic molecular wave function $\Psi_{\mathrm{el}}(\mathrm{r})$. This wave function depends explicitly on the $3N$ coordinates of all N electrons, all of which might undergo positional permutation due to repulsive Coulomb interaction. A first approximation to the challenging task of solving the TISE slackens the interaction between electrons by any exchange and thus reduces the function $\Psi_{\mathrm{el}}(\mathrm{r})$ of $3N$ variables to a product of N functions ϕ each depending only on three variables, $\Psi_{\mathrm{el}}(\mathrm{r}) = \Pi_{\mathrm{i}=1,\mathrm{N}}\phi_{\mathrm{i}}(\mathrm{r}_{\mathrm{i}})$. Atomic orbitals are conveniently chosen to represent the functions ϕ. However, such a *Hartree* product of atomic orbitals violates the Pauli exclusion principle due to the fermion nature of electrons, and hence the appropriate form for a system of noninteracting electrons is a single determinant $|\phi_1(\mathrm{r}_1), \ldots \phi_n(\mathrm{r}_n)|$, known as *Slater* determinant. Such a wave function, from the mathematical properties of determinants, is antisymmetric with respect to exchange of two sets of electronic variables as it should be.

One row of a *Slater* determinant carries contributions from all atomic orbitals ϕ and is commonly referred to as molecular orbital (MO) $\psi\psi^{MO}$. This approximate method for the determination of the ground-state wave function and ground-state energy is the well-known Hartree–Fock (HF) method.

Although in the HF method the electrons obey exchange as required by the Pauli exclusion principle, the electrons are noninteracting, and the movement of one electron within the system is independent from the movement of all other electrons. However, as the presence of Coulomb repulsion between electrons would suggest, the electrons move in a correlated fashion. In order to allow for electron correlation, configuration interaction (CI) is introduced in that the wave function is constructed as a linear combination of several *Slater* determinants, obtained from a permutation of electron occupancies among all MOs available. Increasing the number of *Slater* determinants increases the accuracy of the calculations, although the added accuracy comes with the price of added computational cost that often becomes the limiting factor for WFT calculations.

This brief exposition brings about two main differences between DFT and WFT. A WFT calculation in general, and increasing the accuracy of WFT calculations in particular, is computationally demanding. DFT seems to be more cost-efficient; after all, the simplest HF wave function $\Psi_{el}(r)$ depends on $3N$ spatial coordinates, whereas the probability distribution of electrons in space $\rho(r)$ depends only on three coordinates. But there exist strategies how the result of WFT can be systematically improved, whereas there is no methodical, standardized scheme to improve DFT calculations. In the following, we will explore reasons for the WFT–DFT differences.

In WFT, atoms and molecules constitute the basic systems of interest. Since the distribution and redistribution of electrons within atoms and molecules are central to chemical properties and reactivity, we now limit ourselves to systems comprised of N electrons in motion, with some two-particle interaction. The Hamiltonian of such a system reads $H = T + U + V$, where T and U denote the operators for kinetic energy and for electron–electron interaction energy, respectively. Whereas U results in the *internal* potential energy of our system, the moving electrons might in addition interact with an *external* potential, and the operation V recovers the potential energy due to this extra interaction. For systems of electrons that move in a field of fixed nuclei, the external potential V is always just the nuclear field. Systems of electrons in combination with fields of fixed nuclei represent the essential building blocks of matter such as molecules or solids. For a chemist, it might appear counterintuitive that nuclei, being an essential part of a molecule, represent an *external* potential, but the nuclear potential – although internal to a molecule – is external to the density of the moving electrons.

If we consider the external potential to be a uniformly distributed background positive charge, we arrive at the uniform or homogeneous electron gas (UEG or HEG), also known as jellium. At zero temperature, the properties of jellium depend solely upon the constant electron density distribution $\rho(r)\{= const.\}$. Such a treatment of electronic density, the Thomas–Fermi (TF) model, constitutes the origins of

DFT (Parr and Yang 1989). The TF model is able to describe the kinetic energy of the UEG as functional of the electronic density, and later on Dirac added a density functional for the exchange energy as a conclusion of the Pauli principle. The UEG formalism itself provides the basis for the local density approximation (LDA).

Before we proceed, we take a small step back to WFT. At the beginning of the 1950s, Slater (1951) described the then current situation in WFT as follows: "The Hartree-Fock equations furnish the best set of one-electron wave functions for use in a self-consistent approximation to the problem of the motion of electrons in the field of atomic nuclei. However, they are so complicated to use that they have not been employed except in relatively simple cases." Facing the decision "Do you want to calculate it, or do you want it to be accurate?," Slater decided to replace the peculiar exchange term in the HF equations by something equivalent, yet easier to calculate. Slater used the free-electron approximation for the exchange potential, which, as Dirac has shown, could be expressed as a density functional. His new method, termed HFS, "was easy enough to apply so that we can look forward to using it even for heavy atoms" (Slater 1951), and in order to check its applicability, he performed calculations for the transition metal ion Cu^{+}. The exchange potential functional derived from the exchange energy functional contains one additional, scalable parameter α, which led to the development of the $X\alpha-$ method. This model enjoyed a significant amount of popularity among physicists and is still a topic of ongoing research activities (Zope and Dunlap 2006). The HFS – or the $X\alpha-$ method – became the first practically used DFT method in chemistry.

Two points that were fundamental for the progress of DFT were already anticipated within the advancements of the HFS – or $X\alpha-$method: (1) Every density functional method to some degree contains one or more empirical parameters. Therefore, DFT has often been regarded as "Yet another Semi-Empirical Method" (YaSEM). The Hartree–Fock–Slater model, which can be regarded as ancestor of modern DFT, is such an example. But whereas the HFS method is *intrinsically* approximate, modern DFT is in principle exact (Kohn et al. 1996). (2) Transition metal chemistry has played and continues to play a major role in the progression of DFT. The work of Baerends and Ros (1978) is representative of the transition-metal–HFS era, and Ziegler's contributions, summarized in his early review article (Ziegler 1991), have provided the impetus that changed the perception of calculations based on densities from YaSEM to DFT, "Das Future Tool." A review article by Cramer and Truhlar (2009) is dedicated solely to developments and progress of DFT for transition metal chemistry and summarizes the state of affairs at the end of the first decade of the new millennium.

At the heart of modern DFT is the rigorous, simple lemma of Hohenberg and Kohn (1964), which states that the specification of the ground-state density, $\rho(r)$, determines the external potential V(r) uniquely (Eq. 1):

$$\rho\,(r) \rightarrow V\,(r)\ (\text{unique}) \tag{1}$$

This first theorem by Hohenberg and Kohn (HK-I) is not difficult to prove (Parr and Yang 1989), but for a chemist, the essentials of HK-I that given a

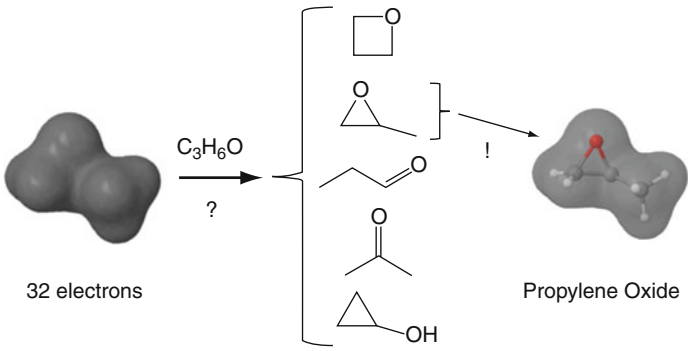

Fig. 1 Visualization of the first Hohenberg–Kohn theorem (density map drawn for a contour envelope of 0.01 a.u.)

density, only one external potential corresponds to that density, are intuitively clear. A pictorial representation of HK-I is shown in Fig. 1; we consider the density created by 32 electrons that move around the external potential created by one oxygen, three carbon, and six hydrogen nuclei. By inspection of a density map of a certain density value, it becomes obvious that of all the atomic constellations considered, only one seems to be consistent with the shape of the density map. Such a consideration reflects ideas developed in the context of "conceptual DFT" (Geerlings et al. 2003).

HK-I also expresses the fact that there is a one-to-one mapping between the potential V(r), the particle density ρ(r), and the ground-state wave function Ψ_0 (Eq. 2):

$$\rho(r) \longleftrightarrow \mathrm{V}(\mathrm{r}) \longleftrightarrow \Psi_0 \tag{2}$$

This implies that all properties of a system are functionals of the ground-state density, since any property may be determined as the expectation value of the corresponding operator. With the help of this lemma, a minimal principle for the energy as functional of ρ(r) can be derived. The second Hohenberg–Kohn theorem (HK-II) provides the necessary guidelines to obtain the ground-state energy. Following HK-II, a variational principle is established, according to which the ground-state density of a system of interest can be determined.

In order to put the promise of the HK theorems that all properties of a system can be obtained from its ground-state density, into reality, one would need a construction that is computationally accessible while maintaining the formal exactness of HK-I and HK-II. To this end, Kohn and Sham (1965) introduced a fictitious system of *N* noninteracting electrons that have for their overall ground-state density the same density as some real system of interest where the electrons do interact. Using some aspects of HF theory, the ground-state wave function Ψ_0 of such a noninteracting system is described by a single *Slater* determinant. The orbitals, which form this

Slater determinant, known as Kohn–Sham (KS) orbitals φ^{KS}, are solutions of N single-particle equations. Following the variational principle, the ground-state energy and the ground-state density are determined from variations in φ^{KS}.

The essential contribution to the KS energy comes from the so-called exchange-correlation energy E_{XC}. It incorporates corrections to the kinetic energy due to the interacting nature of the electrons of the real system, *all* nonclassical corrections to the electron–electron repulsion, as well as electron self-interaction corrections. If E_{XC} is ignored, the physical content of the theory becomes identical to that of the *Hartree* approximation. Thus, within the KS formalism, the electronic energy of the ground state of a system of N electrons moving within an external potential of nuclei is expressed – without approximations – as a functional of the ground-state density (Eq. 3):

$$E[\rho] = T_s[\rho] + U[[\rho(1), \rho(2)]] + V_{ne}[\rho] + E_{XC}[\rho] \tag{3}$$

In Eq. 3, the first term represents the kinetic energy of the system of N noninteracting electrons, the second term corresponds to the Coulombic repulsions between the total charge distributions at two different positions within the system, and the third term accounts for nuclear–electron interactions, due to the presence of an external potential. It is the fourth term, the functional for the exchange-correlation energy E_{XC}, which is responsible for the power and magic of DFT. What makes current DFT applications approximate is the unknown analytic expression of E_{XC}, for which an approximation is needed.

The KS formalism is closely related to the HF formalism. What differentiates the KS operator from the HF operator is the exchange-correlation potential V_{XC}. V_{XC} in turn is a functional derivative of the exchange-correlation energy E_{XC}. Furthermore, the Hamiltonian H operating on the wave function that is associated with the density of a fictitious system of N noninteracting electrons can be expressed as sum of one-electron operators.

Whereas increasing the accuracy of HF calculations is accompanied with a steep increase in computational cost, increasing the accuracy of DFT calculations apparently requires modifications in V_{XC}, which – if at all – only lead to a moderate increase in computational cost. However, whereas it is well known how to systematically improve the accuracy and quality of HF calculations, no comparable strategy exists for DFT calculations within the confines of a KS approach. It appears that a detailed knowledge of the exchange-correlation energy E_{XC} is essential for designing more accurate density functionals.

Holes and Electron Pairs

The exchange-correlation energy E_{XC} is a relatively small part of the total energy of a typical system, although it is by far the largest part of "nature's glue" that binds atoms together (Kurth and Perdew 2000). It arises because the electrons do not

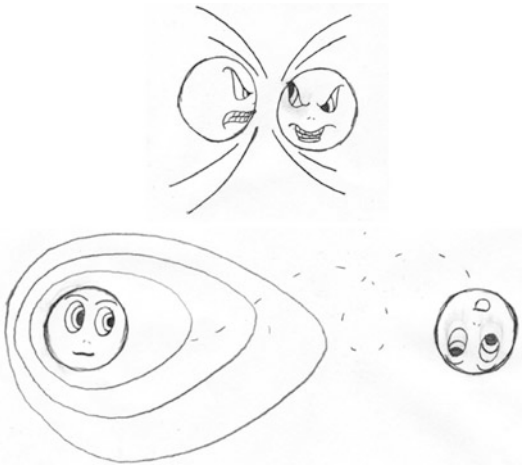

Fig. 2 Electrons in distress: While trying to maximize the attraction from the nuclei, an electron experiences enhanced repulsion from the other electron as it moves around in the molecular framework (*top*). To minimize the repulsion, each electron creates an exclusion area around itself, into which no other electron can penetrate (*bottom*) (Cartoon by Lauren Bertolino)

move randomly through the density but avoid one another. Ziegler (1995) illustrates the situation as follows: An electron will try to maximize the attraction from the nuclei and minimize the repulsion from the other electrons, as it moves around in the molecular framework. To do so, it creates an exclusion area or "no-fly zone" around itself into which no other electron can penetrate, as pictorial exemplified in Fig. 2. The exclusion zone is referred to as the exchange and correlation (XC) hole, and it is the way in which the XC hole is modeled that distinguishes one electronic theory from another. Each density functional has its own characteristic XC fingerprint.

The XC hole also determines to a large part E_{XC}, which however contains *three* different contributions. The first is the potential energy of exchange, which also should include corrections for self-exchange or self-interaction. The second is the potential energy of correlation due to the effect of Coulomb repulsion. Both potential energies are negative and determined by the nature of the XC hole. The third contribution to E_{XC} is a smaller positive kinetic energy of correlation due to the extra swerving motion of the electrons as they avoid one another (Perdew et al. 2009).

The XC hole arises from an extension of the concept of the unconditional one-electron probability density $\rho(1)$ by considering pairs of electrons and a resulting conditional probability. When a reference electron is known to be at position 1, the conditional probability $\rho^{\mathrm{cond}}(2,1)$ of the other electron to be at position 2 can be written as the sum of the unconditional probability $\rho(2)$ of the other electron and the XC-hole density $\rho^{\mathrm{XC-hole}}(2,1)$. Thus, the hole $\rho^{\mathrm{XC-hole}}(2,1)$ describes how the conditional density of the other electron deviates from its unconditional density $\rho(2)$.

It is instructive to have a closer look at hole profiles, and as simple example, we will consider the hydrogen molecule H_2 with only two electrons or one electron pair. In Fig. 3, hole densities for H_2 are shown; the two nuclei H_A and H_B are separated by 72 pm, and the reference electron is placed 15 pm to the left of nucleus H_B.

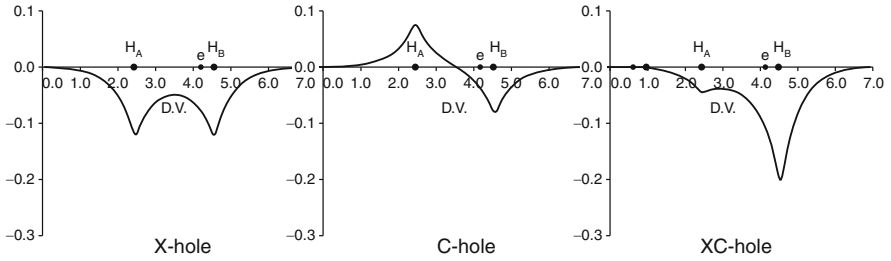

Fig. 3 Hole densities in the hydrogen molecule: Only the full XC-hole $\rho^{\mathrm{XC-hole}}(2,1)$ has physical meaning (Adapted from Baerends and Gritsenko (1997), with permission by the American Chemical Society)

The XC hole can be split into contributions from the exchange or X hole, which arises from the fermion nature of an electron obeying the Pauli principle and the correlation or C hole due to Coulomb repulsion within the pair of electrons. [The X hole and C hole are often referred to as Fermi hole and Coulomb hole, respectively.]

The X hole puts an emphasis on the reference electron. It creates a taboo zone for the other electron with a negative $\rho^{\mathrm{X-hole}}(2,1)$ probability density not only around the region in space where the reference electron currently *is* but also where it *might be*. Regions in the vicinity of both nuclei H_A and H_B are declared as "no-fly zone." The C hole on the other hand puts an emphasis on the other electron. It excludes regions where the other electron might experience Coulomb repulsion with the reference electron, but it also maps out regions where the other electron can benefit from attractive Coulomb interactions with nuclei. We see a negative $\rho^{\mathrm{C-hole}}(2,1)$ probability density around H_B but a positive $\rho^{\mathrm{C-hole}}(2,1)$ probability, a buildup of density, around H_A far away from the reference electron. Whereas the X hole and C hole illustrate exchange and correlation, only the combined XC hole has physical meaning.

Before we continue, a short remark on the use of some language is in order. Since the terms *local* and *nonlocal* are often recurred to in the context of DFT, and often with different meanings, we briefly define how the terms *local* and *nonlocal* are used in this work. An approximation is said to be *local* if its energy density and related properties at any position of interest depend only on the electron density neighborhood of the given position. Otherwise, an approximation is said to be fully *nonlocal*. [We note that some physicists separate local approximations into "strictly local" and "semilocal."]

From an inspection of Fig. 3, it appears that both the C hole and the X hole are inherently nonlocal (the same as the HF exchange energy). The XC hole, too, must therefore be nonlocal, but its dominant contributions arise from the region around its reference electron – the XC hole appears to be more local and less nonlocal than the X or C hole. This observation already anticipates that local density functionals might be able to produce approximate models for the nonlocal XC hole.

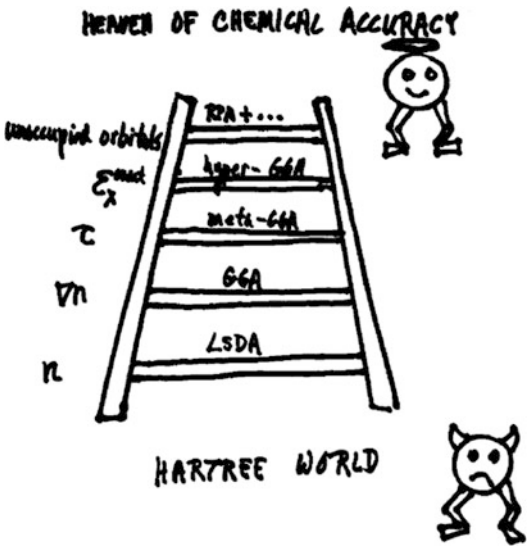

Fig. 4 The Jacob's ladder of density functional approximations to the exchange-correlation energy (Reprinted from Perdew *et al.* (2009), with permission by the American Chemical Society)

Although it seems that there exists no systematic approach like in WFT to improve the accuracy of DFT, the advancement of density functionals depends on more precise descriptions not only of the XC hole but also of the exchange-correlation energy E_{XC}. This task can be approached in a methodical manner.

Climbing Jacob's Ladder

Perdew and Schmidt (2001) compare the development of enhanced density functionals to a climb of Jacob's ladder, leading the way from the *Hartree* world to the heaven of chemical accuracy, illustrated in Fig. 4. Each rung of the ladder adds a refinement to the approximation of the exchange-correlation energy.

First Rung: The Local Density Approximation

The first rung employs only the local densities in the description of the exchange-correlation energy. This method is known as the local density approximation (LDA). [Although vital to the fermion nature of electrons, so far we have treated spin rather novercal. But the issue of spin can be treated as well in density functional theory, and the local spin density approximation (LSD or LSDA) replaces the spin-averaged energy density with the energy density for a polarized homogeneous electron gas. LDA and LSDA are now often used synonymously.]

LDA takes its densities from the uniform electron gas (UEG), and an analytical form of a density functional for the exchange energy of the UEG can be derived (the same exchange energy as used in the HFS method). No such expression exists for the correlation energy, but the UEG correlation energy can be calculated numerically

and fit in various ways. One successful and popular parameterization comes from the work of Vosko, Wilk, and Nussair, referred to as VWN (Vosko et al. 1980).

LDA performs surprisingly well in predicting molecular properties that are based on relative energy differences within a given density. Molecular geometries for representative main group compounds could be reproduced in close agreement to the experiment (Versluis and Ziegler 1988). For transition metal complexes, metal–ligand separations are slightly underestimated, but still within acceptable conformity with X-ray data (Ziegler 1995). However, properties that are based on absolute energy differences between densities, such as bond energies, are not well described by LDA, where a clear overbinding tendency emerged. LDA is therefore a remarkably useful structural, though not thermochemical, tool. The disappointing performance of LDA in estimating thermochemical properties spawned the development of gradient-based methods, the second rung on Jacob's ladder.

Second Rung: The Generalized Gradient Approximation

The second rung or generalized gradient approximation (GGA) adds the gradients of the local densities to the exchange-correlation picture. It became clear that the homogeneous electron gas is only of limited use as a model of the inhomogeneous electron density within molecules, and approximations for exchange and correlation energy were augmented by density gradients. [In the older literature, GGAs are sometimes called nonlocal (LDA/NL), since the gradient implies a directional change within the density.] Two early models for correlation (Perdew 1986) and exchange (Becke 1988a) in combination resulted in the BP86 functional, the GGA that was most influential in the early developments of transition metal DFT (Ziegler 1991). Gradient corrections are essential for a quantitative estimate of bond energies as well as metal–ligand bond distances (Ziegler 1995).

Third Rung: Meta-Functionals

The third rung adds the kinetic energy density to the description of density functionals (Tao et al. 2003) and addresses the smaller third contribution to E_{XC}. Such functionals are referred to as meta-functionals and, when built on second rung functionals, as meta-GGA (MGGA).

The first three rungs of Jacob's ladder all represent local functionals. They often work because of proper accuracy for a slowly varying density or because of error cancellation between exchange and correlation. Error cancellation can occur because the exact XC hole is usually more localized around its reference electron than the exact X hole (compare Fig. 3). Regions in which no error cancellation is expected are regions where exchange dominates correlation (Perdew et al. 2009).

Climbing up the ladder, the approximations become more complicated, more sophisticated, and typically more accurate. Computation times increase modestly from the first to the third rungs and much more steeply after that. The added ingredients on each higher rung of the ladder can be used to satisfy more exact constraints or to achieve better agreement with experimental data (or both). These two strategies define the nonempirical and semiempirical approaches commonly

used to improve density functionals. Beginning with the fourth rung, the nature of the density functionals changes from local to nonlocal.

Fourth Rung: Hyper-Functionals

The fourth rung, which also represents the first fully nonlocal rung, adds the exact exchange energy density. Such a functional is termed hyper-GGA (HGGA). After reaching the second rung, DFT progressed rapidly and took one giant step from the second to the fourth rung, omitting meta-GGAs. Following the idea of adiabatic connection, Becke derived a functional for exchange, which contained contributions from the exact HF exchange (1993a). He then designed an advanced functional for the exchange-correlation contribution containing three parameters for its various parts, including gradient corrections for correlation, gradient corrects for exchange, as well as an exact exchange contribution (1993b). These semiempirical coefficients have been determined by a linear least-square fit to 56 atomization energies, 42 ionization potentials, eight proton affinities, and ten first-row total atomic energies. Becke's functional, combining HF theory and DFT with the use of three empirical coefficients, was the first example and initiated the evolution of so-called hybrid functionals. The hybrid functional B3LYP, based on Becke's parameterization, was to a large part responsible for the meteoric ascent of DFT during the 1990s.

While the first three rungs of Jacob's ladder require no fitting of experimental data, empiricism seems unavoidable on the fourth rung. This has caused some skepticism, and it appeared that the success of "empirical DFT" would eventually be responsible for the death of "true DFT." Gill humorously described the situation at the beginning of the new millennium in his obituary to DFT (Gill 2001). The Jacob's letter metaphor puts the addition of exact exchange to density functionals into proper perspective.

The step from the third rung to the fourth rung results in a new class of functionals, so-called HMGGAs. HMGGA functionals are currently a field of active development and appear to produce promising results. M06, for example, is a HMGGA with good accuracy for a variety of different chemical applications ranging from transition metals over main-group thermochemistry to barrier heights of chemical reactions. Thus, HMGGAs might be considered as a class of density functionals with broad applicability in chemistry (Zhao and Truhlar 2008a). Whether HMGGA is read as hybrid meta-GGA or hyper meta-GGA is a matter of taste; fortunately, both specifications result in the same acronym.

Fifth Rung

The fifth rung of Jacob's ladder adds exact correlation as new ingredient. One might think of this as an expansion of the density space of a system by adding virtual densities into the picture. One approach to this problem is the use of the random-phase approximation (RPA). RPA in DFT in turn is closely related to time-dependent DFT (TD-DFT). The essence of RPA might be described as constructing the excited states of a system as a superposition of particle-hole excitations.

When building a fifth-rung density functional for the exchange-correlation energy, the RPA utilizes full exact exchange and constructs the correlation with the

help of the unoccupied Kohn–Sham orbitals. Like the first three rungs of Jacob's ladder, the fifth rung requires no fitting. Although the essentials of RPA originated in the 1950s, fifth-rung methodologies were considered too computationally expensive for widespread use and application. Yet improvements in hardware and algorithms also entered the development of RPA technology, and it seems that "RPA has the potential to become a building block of future generations of electronic structure methods" (Furche 2008).

In the early days of modern density functional theory, hazy clouds of ambiguity that enfolded the XC hole obscured the view of Jacob's ladder. The existence of the third rung of Jacob's ladder was recognized before the fourth rung entered the Jacob's ladder picture (Becke and Roussel 1989), but at first it did not appear as a safe and secure stage for the ascent toward the heaven of chemical accuracy. Thus, although MGGAs predate HGGAs, the computational development of HGGAs predates that of MGGAs. Only after the clouds of ambiguity lifted, MGGAs became a recognized DFT approach in computational chemistry, and HMGGAs began to appear.

The Jacob's ladder scheme is not the only way to arrive at exact functionals. When leaving the confines of ordinary KS-DFT methods, and using ideas from WFT, one arrives at ab initio density functional theory, the seamless connection of DFT and WFT (Bartlett et al. 2005). While these methods have not yet positively established themselves as standard approaches in computational chemistry, the fundamental conception that guided the way to the fourth rung – capturing the best of both worlds – marks the beginning of ab initio DFT and led to the notion of double-hybrid theory (Grimme 2006a), in which DFT calculations are supported not only by exact exchange but also by HF correlation. Along the same lines, range-separated functionals (Leininger et al. 1997) base their decision on how to deal with electron–electron correlation – the DFT or WFT way – on the central variable that describes a pair of electrons. The idea also found its entry into the realm of exchange (Tsuneda and Hirao 2014), and at the time of writing, it appears that the offspring of parent functionals is ever more growing in number.

Practical DFT and the Density Functional Zoo

A practical DFT-based calculation is in many ways similar to a traditional HF treatment in that the final outcome is a set of orbitals, the Kohn–Sham orbitals φ^{KS}. The KS orbitals are often expanded in terms of a basis set as in the traditional linear combination of atomic orbital (LCAO) approach of traditional HF methods. Most often, Gaussian-type basis functions are used to construct atomic orbitals (GTO). A major exception is the Amsterdam Density Functional (ADF) suite of programs, where Slater-type basis functions (STO) are used. ADF constitutes one of the first programs developed essentially for applications of DFT.

The evaluation of matrix elements of the Kohn–Sham exchange-correlation potential always requires at some step a 3-day numerical integration. Solutions to the problem of carrying out 3D numerical integration for polyatomic systems to

arbitrary precision (Becke 1988b) provided a major thrust for computational DFT, and proficient improvements were made in connection with developments of the ADF computer code (Boerrigter et al. 1988). The availability of economical numerical integration schemes made the choice of STOs over GTOs computationally compatible.

The local nature of the effective potential in the one-electron Kohn–Sham equations affords efficient computational schemes. During the development of ADF, the remaining Coulomb problem, the two-electron-integral "bottleneck," has been addressed by the introduction of auxiliary basis sets, the so-called density fitting (Baerends et al. 1973).

Many of the pioneering improvements made during the development of the ADF suite of programs have become standard tools in density functional calculations, and as a result, DFT calculations perform compatible to, if not better than HF methods. We note that a density fit is not possible, when the chosen functional utilizes exact exchange.

By now, a plethora of density functionals is available for electronic structure calculations. Toward the end of the first decade of the new millennium, Sousa and coworkers have presented an authoritative review, in which they evaluate the performance of over 50 different density functionals (Sousa et al. 2007). The authors also report the percentage of occurrences of the names of different functionals in journal titles and abstracts; we interpret these numbers as measure for usage and popularity of the corresponding functional. Although new functionals appear every year, the popularity ranking seems to possess some stability within a time interval of several years. Thus, in Fig. 5, we have compiled data for the seven most popular functionals, taken from the work of Sousa and coworkers, and include a popularity pie chart as well.

FUNCTIONAL (YEAR)	TYPE	USAGE
B3LYP (1994)	HGGA	80 %
BLYP (1988)	GGA	5 %
B3PW91 (1993)	HGGA	4 %
BP86 (1988)	GGA	3 %
PBE (1996)	GGA	2 %
BPW91 (1991)	GGA	1 %
TPSS (2003)	MGGA	1 %

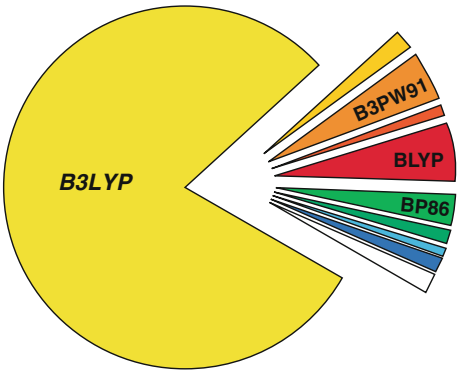

Fig. 5 Most popular density functionals at the end of the first decade of the new millennium (Data based on results of extensive literature searches (Sousa et al. 2007))

The key information conveyed in Fig. 5 is the fact that B3LYP is by far the most popular density functional in chemistry, representing 80 % of the total of occurrences of density functionals in the literature, in the period 1990–2006 (Sousa et al. 2007). Other popular density functionals such as BLYP, B3PW91, and BP86 acquire usage shares of 5 % and less and can only be considered as also-rans in the functional race.

It seems advisable to briefly talk about how to decipher the density functional code. With the advent of GGAs at the end of the 1980s, the abbreviation for each GGA functional usually consisted of two parts: the first for exchange and the second for correlation. As an example, BP86 takes its exchange contribution from the work of Becke (1988a) and correlation from the work of Perdew (1986). Similarly, BLYP breaks down into B exchange and LYP correlation. Later, when gradient corrections for exchange and correlation were often taken from the same work, the functional is usually referred to by one combined code only. The GGA functional PBE takes its gradients for exchange as well as for correlation from the work of Perdew, Burke, and Ernzerhof. The same holds true for the MGGA TPSS. Strictly spoken, the PBE functional should be referred to as PBEPBE. It is also possible that the individual parts are combined with other functionals, for example, PBELYP or BPBE. HGGAs usually contain one number that indicates the degree of parameterization when building the hybrid: B3LYP refers to a three-parameter mixing of B exchange, LYP correlation, and exact exchange, whereas B1LYP refers to a one-parameter hybrid density functional. As density functionals get more elaborate and more complex, the XC coding is not always strictly followed. The HMGGA M06 and its variations (M06-L, M06-2X, M06-HF), for example, refer to a set of functionals developed at the University of Minnesota in 2006.

The pie chart presented in Fig. 5 bears a striking resemblance to *Pac-Man*. Like the arcade game *Pac-Man*, often credited with being a landmark in video game history and virtually synonymous with video games, B3LYP has to be considered a landmark in electronic structure theory and is often used as a synonym for DFT. However, the same as there is more to video games than just *Pac-Man*, there is more to density functional theory than just B3LYP. In section "DFT: Computational Chemistry in Action," we will explore the characteristics and capabilities of density functional in more detail.

The reader, who would like to know more about the details and derivations of DFT, will find valuable information about the basics in the *A Chemist's Guide to Density Functional Theory* (Koch & Holthausen 2002) and will learn more about advanced aspects in the *A Primer in Density Functional Theory* (Fiolhais et al. 2003).

DFT: Computational Chemistry in Action

The breakthrough of DFT coincided with a rise of computational power at the end of the last millennium. CPU architectures advanced from CISC to RISC designs, supercomputers transformed from single vector processors to computing clusters.

However, as the computational power increased, the problems too became more and more demanding, and the molecules that found their way into input files for density functional programs grew bigger and bigger. Computing time remains to be a crucial factor when assessing the performance of computational methods, and linear-scaling approaches are one of the great strengths of DFT (Yang 1991). However, these techniques fall out of the scope of our review and assessment, and we begin with a comparison of computational demands of representative density functionals, following standard approaches.

Computational Performance

We start this section remarking that there is not something like "the best functional and basis set for all properties." Rather, the specific methodological approach to be used depends from the specific problem at hand. Nevertheless, many functionals are robust enough to give rather reasonable results in a large series of chemical properties, and the scope of this section is to provide an overview of the performances of typical functionals and basis sets, trying to highlight which ones perform remarkably better or remarkably worse than the average, if this is known. Further, as a practical *vademecum*, the scope of this section is to give an overview of performances under "standard working conditions." Thus, the focus will be on performances that can be expected when working with real-size systems (50–100 atoms including a transition metal), which requires a compromise between the computer resources available and the combination of functional and basis set used, rather than peak performances that can be reached with a sophisticated last-generation functional in combination with a very extended basis. On the other hand, there are several excellent reviews that provide an accurate and critical assessment of the various methods, with a particular focus on the best performances that can be achieved, independently from the computational cost (Sousa et al. 2007; Cramer and Truhlar 2009). Methods that currently are computationally too expensive might become the standard computational tools in the future.

Finally, the number of possible functionals is very large, so that it is more confusing than enlightening to review all of them. In addition, it might well be that the best functional for a specific problem has not been tested in the several benchmarking studies published in the literature. As a general rule, before wasting huge amounts of computer power with the wrong functional and/or basis set, it is wiser to invest some time to read the literature to find which computational method works better (or acceptably well) for a given problem and possibly have a feeling of the accuracy through test calculations on small selected systems.

To give an idea of the relative cost of the various functionals, the relative computational time required by some functionals in two standard applications such as the calculations of the energy and of the first derivatives of the energy with respect to the atomic coordinates (which must be calculated at each geometry optimization step) and the calculation of the second derivatives of the energy with respect to the atomic coordinates (which must be calculated for vibrational analysis) is reported

Table 1 Relative performance of various functionals, as implemented in the Gaussian 09 package, in the calculation of energy and gradients, or second derivatives, for an organometallic complex of formula $RuC_{31}H_{33}Cl_2N_3$

		E + gradients	2nd derivatives	E + gradients
Method		SVP		TZVP
BP86 (density fit)	GGA	1.0	1.0	1.6
BP86	GGA	1.5	1.9	4.1
PBE	GGA	1.5	1.8	4.2
B3LYP	HGGA	2.6	2.9	8.9
PBE1PBE	HGGA	3.0	3.2	9.2
TPSS (density fit)	MGGA	1.6	1.9	2.6
TPSS	MGGA	2.1	2.3	5.1
TPSSh	HMGGA	3.5	3.5	9.4
M06	HMGGA	3.6	4.0	10.6

in Table 1. The system considered in these calculations is a 70 atom Ru complex whose brute formula is $RuC_{31}H_{33}Cl_2N_3$.

The data reported in Table 1 clearly indicate that GGA calculations are computationally very effective. In addition, for DFT methods that do not rely on exact exchange, the performance can be further improved by using an auxiliary basis set to fit the electron density (usually called density fit or resolution of identity). Indeed, without this technical setup, the same GGA or MGGA functional – compare the BP86 (density fit) and the simple BP86 values in Table 1 – is roughly 50 % slower. The same consideration applies when MGGA functionals are considered; compare the TPSS (density fit) and the simple TPSS values in Table 1. We note that this technical acceleration is not possible when the Hartree–Fock exchange must be evaluated, and thus HGGA and HMGGA calculations cannot benefit from it. Generally speaking, there are marginal differences within a family of functionals, and HGGA functionals are roughly 2–3 times slower than GGA functionals. MGGA functionals, particularly when the resolution of identity technique is invoked, are roughly 50 % slower than GGA functionals and thus are quite faster than HGGA functionals. HMGGA functionals are roughly 3–4 times slower than GGA functionals. This relative speed between the different families of functionals is maintained when second derivatives are evaluated. Moving to the effect of the size of the basis set, calculations performed with a triple-ζ plus one polarization function of main group atoms results in an increase of the required computational time by a factor of 2–3 roughly. Thus, on going from an accelerated GGA functional in combination with a split valence plus one polarization function basis set, to a HMGGA functional in combination with a triple-ζ plus one polarization function, basis set result in an increase of the computational time by a factor of 10 roughly. In other words, a GGA/SVP calculation that would take one day would require more than one week, roughly, if performed at the HMGGA/TZVP level. This indicates that the selection of the most appropriate computational method (both functional and

basis set) must be a trade between the accuracy needed and the computational time (or power) available. Of course, degradation of accuracy below the level required by the specific problem at hand is not possible.

Properties of Molecular and Electronic Structure

To explore the capabilities of various density functionals, we have selected twelve representative properties of atoms and molecules. We begin with molecular structure (bond lengths, bond angles, vibrational frequencies) and basics of electronic structure (electron affinities and ionization potentials). We then proceed to the energetics of transformations of molecules (atomization energies, heats of formation, energy barriers), which will carry us to chemical bonding. The nature of the chemical bond remains a central theme in theoretical chemistry, and we discuss regular bonds as well as weak bonds, all being at the focus of ongoing research activities (bond energies, hydrogen bonding, weak interactions). The issue of spin in DFT deserves particular attention (spin states). Although DFT essentially is a ground-state theory, excited states too can be treated with density functional theory, and with our last property we briefly touch this topic (excited states). Time-dependent density functional theory (TD-DFT) is a topic in its own right, and an appropriate coverage of TD-DFT falls out of the scope of the present work. The reader will find an entry into this excited field when studying the articles compiled by Marques and coworkers (2006).

The twelve topics we selected in no way exhaust the capabilities of DFT, and any property that can be treated with WFT is in principle accessible with DFT as well. As an example, we refer the reader to a most instructive review by Neese (2009) that illustrates the capabilities of DFT in the field of molecular spectroscopy.

When evaluating the performance of computational methods, benchmarking is an essential procedure in which calculated properties are evaluated against accurate experimental data. By now, a large number of problem-specific databases have been established, which cover a wide variety of different physicochemical properties, such as proton affinities, atomization energies, barrier heights, reaction energies, and spectroscopic properties. However, these databases are not free from chemical biases and often narrowed by the structural space of chemical intuition. There is always the risk that when following established procedures, benchmark studies might lose some of their general appeal. As to avoid the dangers of casual benchmarking, Korth and Grimme have developed a “mindless” DFT benchmarking protocol. Here, the databases consist of randomly generated molecules that rely on systematic constraints (Korth and Grimme 2009) rather than on what is supposed to be chemical insight.

In the following, we will make extensive reference to published benchmark studies. However, it might well be that a particular molecule of interest to the reader is not covered within one of the existing benchmark databases, and benchmark studies in general provide good starting points for calculations, but no guarantee for correctness.

One: Bond Lengths

It is well established that almost any DFT approach, beyond LDA, is able to reproduce correctly the geometry of molecular systems composed of main group atoms. With the increase of computer resources, it is becoming customary to test the performances of various methods through calculations on a rather large set of molecules and to report statistical values. In one of such comparative studies, 17 closed-shell molecules composed by first-row atoms, for which accurate experimental geometries determined in the gas phase were available, confirmed that the performance of commonly used GGA (BLYP, BPW91, and BP86) and HGGA (B3LYP, B3PW91, and B3P86) is quite accurate, although the mean unsigned error (MUE) on the bond length obtained with the GGA functionals, between 0.015 and 0.020 Å roughly, is slightly larger than that calculated with the HGGA functionals, usually below 0.010 Å (Wang and Wilson 2004). The convergence of the geometry was tested with respect to increasing basis set size from cc-pVDZ to aug-cc-pV5Z and was shown to occur quickly. Convergence is typically reached at the triple-ζ level, and beyond this level minor fluctuations, in the order of 0.002 Å, were observed. Thus, excellent performances require that at least a triple-ζ basis set is used. Similar conclusions were reached in a different benchmark study on a dataset of 44 small molecules (Riley et al. 2007). Again, GGA functionals in combination with Pople basis sets of the 6-31G family result in MUE between 0.015 and 0.020 Å, while HGGA functional results in MUE below 0.010 Å. The MGGA functionals tested resulted in a minor improvement relative to GGA functionals, while the tested HMGGA functionals substantially reproduce the performance of HGGA functionals. This indicates that the advantage of meta-functionals certainly is not in bond distances.

To give an idea of the performance of some popular functionals, and also to show the effect of the basis set, the dependence of the O–H bond length in water is reported in Table 2 as an exemplary case. The data indicate that reasonably accurate bond lengths (within 0.02 Å from the experimental value) can be achieved with computationally cheap GGA functionals and that HGGA performs slightly better with modest basis sets. As a general trend, the HGGA bond lengths are slightly shorter than the corresponding GGA value and independent of the computational approach; slightly shorter bond lengths are predicted with basis sets of increasing quality. It is noteworthy that with the extended aug-cc-pV5Z basis set, the GGA values slightly overestimate the experimental value, whereas the HGGA values slightly underestimate it. Importantly, rather good results can be achieved also with relatively small basis sets, which allow calculating geometries for fairly large systems with a reasonable accuracy.

The very good performance of almost any functional to calculate accurately bond lengths of molecular systems composed by main group atoms is not replicated when bonds to transition metals are considered. Focusing on an extensive benchmark of 42 functionals on a database of 13 metal– ligand bond lengths, the MLBL13/05 database, all functionals provide rather good results, with MUE normally between 0.01 and 0.02 Å when a basis set of triple-ζ quality is used (Schultz et al. 2005a).

Table 2 Performance of selected functionals and basis sets in predicting the experimental value of the O–H bond length of water, 0.956 Å

	BP86	revPBE	B3LYP	TPSS	TPSSh	M06
6-31G	0.985	0.984	0.976	0.983	0.978	0.970
SVP	0.976	0.974	0.967	0.974	0.969	0.963
6-31G(d,p)	0.974	0.973	0.965	0.972	0.967	0.960
TZVP	0.972	0.971	0.962	0.969	0.965	0.958
cc-pVDZ	0.978	0.977	0.969	0.977	0.972	0.964
cc-pVTZ	0.971	0.970	0.961	0.968	0.964	0.958
cc-pVQZ	0.970	0.968	0.960	0.968	0.963	0.956
cc-pV5Z	0.970	0.968	0.960	0.967	0.963	0.956
aug-cc-pVDZ	0.974	0.974	0.965	0.973	0.970	0.961
aug-cc-pVTZ	0.971	0.970	0.962	0.969	0.964	0.958
aug-cc-pVQZ	0.970	0.968	0.961	0.967	0.963	0.956
aug-cc-pV5Z	0.970	0.968	0.960	0.967	0.963	0.956

Extending the benchmark to a database containing the bond length of eight metal–metal dimers, the TMBL8/05 databases, the situation deteriorates. GGA functionals, including the popular BP86, BLYP, and PBE functionals, still provide rather good results, with MUE between 0.02 and 0.03 Å when a basis set of triple-ζ quality is used, while reducing the quality of the basis set to double-ζ deteriorates performances remarkably, with MUE between 0.06 and 0.09 Å (Schultz et al. 2005b). In the GGA family, the HTCH and OLYP functionals, with MUE greater than 0.03 Å, should be avoided. The rather good performance of GGA functionals is not replicated by HGGA functionals, including the popular B3LYP and PBE1PBE functionals, with MUE between 0.08 and 0.09 Å. In the HGGA family, the BH&HLYP and MPW1K functionals, with MUE greater than 0.12 Å, should be avoided. Interestingly, MGGA functionals do not perform as or better than GGA functionals in predicting bond lengths, but rather worse. Indeed, including also the popular BB95 and TPSS functionals, they result in MUE greater than 0.06 Å. Introduction of HF exchange partially improves the performance of MGGA functionals, and the tested HMGGA functionals, including the B1B95 and the TPSSh functionals, result in MUE between 0.03 and 0.07 Å (Schultz et al. 2005a). Finally, the M06 functional performs particularly poor, with a MUE of 0.131 Å (Zhao and Truhlar 2008b).

To give an idea of the performance of some popular functionals in the calculation of the M–ligand distances and of the effect of the metal on the bond distance of the ubiquitous CO ligand, analysis of these distances in three typical binary carbonyl complexes involving first-row transition metals is reported in Table 3.

Basically, all the functionals reproduce the experimental M–CO distances well within 0.02 Å, but many of the functionals tested underestimate the difference in the axial and equatorial Fe–CO distances. In this respect, HGGA and HMGGA functionals seem to perform slightly better, although there is quite a debate on the exact

Table 3 Performance of selected functionals, in combination with the TZVP basis set on all the atoms, in predicting the experimental value of the M–C and C–O bond length (in Å) in three first-row $M(CO)_n$ complexes

		$Ni(CO)_4$		$Fe(CO)_5$		$Cr(CO)_6$	
		M–C	C–O	$M–C_{eq}$, $M–C_{ax}$	$C–O_{eq}$, $C–O_{ax}$	M–C	C–O
Exp.		1.838	1.141	1.803, 1.811	1.133, 1.117	1.918	1.141
BP86	GGA	1.828	1.151	1.809, 1.810	1.157, 1.153	1.910	1.155
PW91	GGA	1.824	1.149	1.805, 1.806	1.154, 1.151	1.906	1.153
revPBE	GGA	1.829	1.150	1.809, 1.810	1.155, 1.153	1.911	1.154
B3LYP	HGGA	1.845	1.137	1.820, 1.828	1.142, 1.138	1.926	1.141
PBE1PBE	HGGA	1.822	1.134	1.796, 1.805	1.140, 1.136	1.900	1.138
B98	HGGA	1.839	1.137	1.813, 1.820	1.142, 1.138	1.915	1.141
TPSS	MGGA	1.830	1.149	1.813, 1.816	1.154, 1.151	1.918	1.152
mPWKCIS	MGGA	1.832	1.150	1.810, 1.811	1.156, 1.153	1.911	1.154
BB95	MGGA	1.833	1.150	1.811, 1.811	1.156, 1.153	1.912	1.154
TPSSh	HMGGA	1.828	1.142	1.809, 1.815	1.147, 1.144	1.915	1.146
M06	HMGGA	1.848	1.133	1.820, 1.821	1.139, 1.135	1.920	1.138

assignment of the Fe–CO distances in $Fe(CO)_5$. Similar good behavior is shown by all the functionals in the prediction of the CO distance when bonded to a transition metal, although the GGA and MGGA functionals tested yield systematically longer CO distances. In this respect, HGGA and HMGGA functionals do perform slightly better.

Two: Bond Angles

The good performance of almost every functional to predict correctly bond lengths of molecular systems composed by main group atoms is confirmed in the case of bond angles. Again, a benchmark study on 17 closed-shell molecules composed by first-row atoms, for which accurate experimental geometries determined in the gas phase was available, confirmed that the performance of commonly used GGA (BLYP, BPW91, and BP86) and HGGA (B3LYP, B3PW91, and B3P86) functionals is quite accurate, with a MUE between 1.0° and 1.5° (Wang and Wilson 2004). Differently from bond lengths, GGA and HGGA methods perform rather similarly on bond angles. Also for bond angles, the convergence was tested with respect to increasing basis set size from cc-pVDZ to aug-cc-pV5Z and was shown to occur quickly, and again convergence is typically reached at the triple-ζ level. Similar conclusions were reached in a different benchmark study on a dataset of 44 small molecules (Riley et al. 2007). All the functionals considered resulted in MUE between 1.0° and 1.5°, independent of the functional used.

To give an idea of the performance of some popular GGA and HGGA functionals, and also to show the effect of the basis set, the dependence of the H–O–H angle in water is reported in Table 4 as an exemplary case. Accurate bond angles (within 1.0° from the experimental value) can be achieved with all functionals and moderate basis sets.

Table 4 Performance of selected functionals and basis sets in predicting the experimental value of the H–O–H angle of water, 105.2°

	BP86	revPBE	B3LYP	TPSS	TPSSh	M06
6-31G	107.2	107.1	108.3	107.1	107.7	109.4
SVP	102.2	102.1	103.1	102.3	102.7	103.3
6-31G(d,p)	103.1	103.0	104.0	103.3	103.7	104.5
TZVP	104.1	104.1	105.1	104.3	104.6	104.9
cc-pVDZ	101.7	101.7	102.7	104.9	102.3	102.8
cc-pVTZ	103.6	103.5	104.5	103.7	104.0	104.4
cc-pVQZ	103.9	104.0	104.9	104.0	104.3	104.8
cc-pV5Z	104.2	104.3	105.1	104.3	104.5	105.0
aug-cc-pVDZ	103.8	103.8	104.8	103.8	104.1	104.7
aug-cc-pVTZ	104.2	104.2	105.0	104.3	104.6	104.9
aug-cc-pVQZ	104.2	104.3	105.1	104.3	104.6	104.9
aug-cc-pV5Z	104.2	104.3	105.1	104.3	104.6	105.1

Three: Vibrational Frequencies

Benchmarking various DFT methods to reproduce accurately vibrational frequencies of 35 molecular systems composed by main group atoms revealed that GGA methods, with a MUE of roughly 40 cm^{-1}, are among the most accurate functionals (Riley et al. 2007). Indeed, the performance of several HGGA methods was at least 20 cm^{-1} worse, with MUE between 60 and 80 cm^{-1}, and meta-functionals are not an improvement. As for other geometrical properties, accurate performance requires that a triple-ζ basis set be used. The GGA functionals also performed better than HGGA functionals in the prediction of the vibrational frequency in nine homonuclear 3d metal dimers, with a MUE around 100 cm^{-1} for BLYP and BP86 and around 120 cm^{-1} for B3LYP and B3P86. Nevertheless, both families of functionals resulted in a rather large deviation from accurate data (Barden et al. 2000).

The performance of various functionals in the prediction of the CO stretching frequency in typical binary carbonyl complexes with first-row transition metals is exemplified in Table 5. Simple GGA and also MGGA functionals perform better and are able to capture the experimental value with an accuracy of roughly 50–100 cm^{-1}, while Hartree–Fock exchange seems to deteriorate results, since the HGGA and HMGGA functionals reproduce the experimental value with an accuracy of roughly 150–200 cm^{-1}. In terms of percent, the GGA and MGGA functionals overestimate the experimental values by 3–4 %, while the HGGA and HMGGA functional by 6–10 %. While these results may seem quite accurate, almost all the functionals considered are unable differentiate too little between metals. In fact, the experimental value decreases by 58.1 cm^{-1} on going from $Ni(CO)_4$ to $Cr(CO)_6$, but the functionals examined are unable to capture this difference. The best performing are the B98 functional, with a difference of merely 15.0 cm^{-1}, and the HGGA and HMGGA with differences slightly smaller than 10 cm^{-1}.

On the other hand, the simple BP86 GGA functional has been also tested in the prediction of the CO stretching frequency in rather large organometallic complexes.

Table 5 Performance of selected functionals, in combination with the TZVP basis set on all the atoms, in predicting the symmetric frequency of the CO stretching mode in selected first-row transition metal binary carbonyl complexes. Next to each calculated frequency is reported the %error calculated as $\%err = 100*(\nu_{Exp.}/\nu_{DFT})$. The final column reports the difference between the $Ni(CO)_4$ and the $Cr(CO)_6$ frequencies

Method		$Ni(CO)_4$		$Fe(CO)_5$		$Cr(CO)_6$		ν_{Ni}-ν_{Cr}
Exp.		2061.3	%err	2038.1	%err	2003.0	%err	58.1
BP86	GGA	2104.0	2.1	2103.0	3.2	2102.0	4.9	2.0
PW91	GGA	2116.0	2.7	2115.0	3.8	2115.0	5.6	1.0
revPBE	GGA	2110.0	2.4	2109.0	3.5	2109.0	5.3	1.0
B3LYP	HGGA	2194.0	6.5	2184.0	7.2	2185.0	9.1	9.0
PBE1PBE	HGGA	2232.0	8.3	2223.0	9.1	2223.0	11.0	9.0
B98	HGGA	2212.0	7.3	2202.0	8.0	2197.0	9.7	15.0
TPSS	MGGA	2121.0	2.9	2116.0	3.8	2117.0	5.7	4.0
mPWKCIS	MGGA	2102.0	2.0	2102.0	3.1	2102.0	4.9	0.0
BB95	MGGA	2100.0	1.9	2100.0	3.0	2100.0	4.8	0.0
TPSSh	HMGGA	2169.0	5.2	2162.0	6.1	2162.0	7.9	7.0
M06	HMGGA	2234.0	8.4	2224.0	9.1	2226.0	11.1	8.0

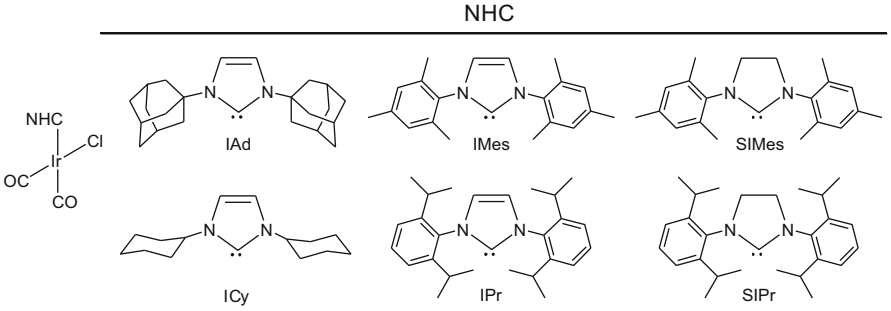

Fig. 6 Iridium complexes that bear N-heterocyclic carbene ligands

For these large and computationally demanding systems, which are displayed in Fig. 6, computationally effective methods are needed.

The data reported in Table 6 clearly show the very good performance of the BP86 functional, which is able to reproduce the higher frequency symmetric CO stretching with an error of roughly 20 cm^{-1} only and the lower frequency asymmetric CO stretching with an error of roughly 30 cm^{-1}. Further, despite the poor performances discussed above in the ability of GGA functionals to differentiate between different binary $M(CO)_n$ complexes, comparison of the saturated N-heterocyclic carbene complexes (SIPr and SIMes) with their unsaturated counterparts (IPr and IMes) indicates that the DFT values reproduce the experimental finding that both CO stretches are about 1 or 2 cm^{-1} smaller in the complexes with the unsaturated N-heterocyclic carbene ligand (Kelly et al. 2008).

Table 6 Experimental and DFT calculated CO stretching frequencies, in cm^{-1}, in several N-heterocyclic carbene complexes

Method	Experimental		BP86	
(IAd)Ir(CO)$_2$Cl	2063.4	1979.8	2082	2010
(ICy)Ir(CO)$_2$Cl	2064.8	1981.2	2083	2015
(IPr)Ir(CO)$_2$Cl	2066.8	1981.0	2083	2005
(SIPr)Ir(CO)$_2$Cl	2068.0	1981.8	2084	2007
(IMes)Ir(CO)$_2$Cl	2066.4	1979.8	2084	2007
(SIMes)Ir(CO)$_2$Cl	2068.0	1981.8	2085	2008

Table 7 Calculated and experimental electron affinities, in kcal/mol, for neutral late transition metal M(CO)$_n$ complexes

System	Experimental	BP86/6-311G(d)	B3LYP/6-311G(d)
Mn(CO)	25.7	25.0	24.0
Fe(CO)	26.7	25.7	21.8
Ni(CO)	18.5	19.1	13.8
Fe(CO)$_2$	28.1	32.6	–
Ni(CO)$_2$	14.8	19.9	16.0
Ni(CO)$_3$	24.8	35.3	27.9

Four: Electron Affinities and Ionization Potentials

A benchmark study of 24 molecules from the G2/97 dataset, with the addition of PO_2, indicated that, with some exceptions, DFT methods reproduce the electron affinity of molecular systems composed by main group atoms with a MUE close to 4 kcal/mol. Some hybrid functionals, such as the B98 functional, performs slightly better (MUE = 3.15 kcal/mol), while GGA functionals with the P86 correlation term usually perform rather poorly, with MUE around 6 kcal/mol (Riley et al. 2007). Finally, meta-functionals are not an improvement. As for any molecular system with a negative charge, the calculation of electron affinity requires that basis set containing diffuse functions are used. Moving to ionization potentials, the performance of the various methods on 36 molecules from the G2/97 dataset, with the addition of PO_2, substantially replicates that found for electron affinities, although the MUE, between 5 and 6 kcal/mol, is slightly larger (Wang and Wilson 2004). The B1B95 MHGGA functional provided the best performance, with a MUE of 4.25 kcal/mol.

Moving to selected cases (see Table 7), the BP86 GGA functional seems quite more accurate than the HGGA B3LYP functional in predicting the electron affinity of highly unsaturated late transition metal M(CO)$_n$ complexes, but the HGGA functional seems to be more accurate when the unsaturation at the metal is reduced (Zhou et al. 2001). These results exemplify the difficulty to extract trends from benchmarks, if the specific case at hand has not been included in the testing dataset.

Five: Atomization Energies

A benchmark study on 17 first-row closed-shell molecules indicated that in the calculation of the atomization energy with the Dunning correlation-consistent basis sets, the HGGA functionals, with a MUE of roughly 2.2 kcal/mol, outperform GGA functionals, such as BLYP (MUE = 7.2 kcal/mol), with BP86 performing particularly bad (MUE = 16.2 kcal/mol) (Wang and Wilson 2004). In another benchmark study on the atomization energy of a dataset composed by 109 main groups of organic and inorganic molecules, calculated with the MG3S basis set, HGGA functionals were again confirmed to perform well, with MUE smaller than 1.0 kcal/mol, while GGA functionals, such as the PBE, with a MUE of 3.0 kcal/mol, again performed poorly. The peak performance of 0.40 kcal/mol was produced with the B1B95 functional, while the classic B3LYP resulted in a MUE of 0.91 kcal/mol. Finally, HMGGA functionals were shown to perform similarly to HGGA functionals (Zhao and Truhlar 2005a). A set of range-corrected functionals, including the CAM-B3LYP, the LC-ωPBE, and the ωB97 family, also performed particularly well, with MUE between 0.51 and 0.89 kcal/mol (Peverati and Truhlar 2014). On the other hand, GGA functionals perform well when the atomization energy of 9 metal dimers in the TMAE9/05 database is calculated, with MUE in the range of 5–8 kcal/mol. HGGA functionals, instead, resulted in MUE around 15–30 kcal/mol, with only the B97-1, B97-2, and B98 functionals with MUE below 10 kcal/mol. MGGA and HMGGA functionals substantially replicate the results obtained with non-meta-functionals, although the M05 and M06 functionals result in the very low MUE of 6.9 and 4.7 kcal/mol, respectively (Zhao and Truhlar 2008b). These results are another indication that hybrid functionals usually perform better for molecules composed by main group atoms, whereas GGA and MGGA functionals perform better for transition metal chemistry.

Six: Heats of Formation

The accurate calculation of this property, even for rather simple molecular systems composed by main group atoms, still represents a challenge for several functionals. Indeed, the MUE on the heat of formation in a benchmark study on 24 molecules from the G2/97 dataset, with the addition of PO_2, spans the rather broad range of 10–30 kcal/mol, even if basis set of rather good quality, such as the 6-31++G* basis set, are used. Functionals to be avoided are those containing the P98 correlation term among the GGA, the B1LYP and the B98 among the MGGA, the PBEKCIS among the MGGA, and the BB1K among the HMGGA. On the other side, good performances were obtained with the PBELYP, PW91LYP, MPWPW91, and MPWPBE GGA functionals, the PBE1PBE and B3PW91 HGGA functionals, and finally the TPSS and the TPSSKCIS MGGA functionals. With these functionals, the MUE on the heats of formation usually is below 10 kcal/mol (Riley et al. 2007). Augmented correlation-consistent Dunning-type basis sets usually lead to slightly better performances. Nevertheless, some computational results have cast a shadow on the common procedure to test heats of formation on small molecules. Indeed, it has been shown that almost all the functionals, including the popular

B3LYP functional, are unable to predict correctly the heats of formation of n-alkanes (Curtiss et al. 1997, 2000). Due to the inability to describe properly long-range attractive dispersion interaction, practically all functionals introduce a systematic error in the calculation of the isodesmic stabilization energy (Eq. 4). This systematic error ranges between 0.90 kcal/mol for the HMGGA MPWB1K functional and 1.82 kcal/mol for the OLYP functional. The BP86 and PBE GGA functionals result in an error of 1.25 and 1.08 kcal/mol, respectively, while the HGGA functional B3LYP results in an error of 1.33 kcal/mol. While these errors may seem to be not dramatic, they are per CH_2 unit, so that the errors are between 10 and 20 kcal/mol for a simple molecule such as *n*-decane (Wodrich et al. 2006).

$$n - CH_3 - (CH_2)_m - CH_3 + m\,CH_4 \rightarrow (m+1)\,C_2H_6 \tag{4}$$

Seven: Energy Barriers

The performance of a series of functionals was tested to reproduce the barrier height for a series of reactions. Starting from hydrogen transfer reactions, the forward and backward barrier for the following 3 reactions $OH\bullet + CH_4 \rightarrow CH_3\bullet + H_2O$, $OH\bullet + H\bullet \rightarrow O(^3P) + H_2$, and $H\bullet + H_2S \rightarrow HS\bullet + H_2$, which constitute the BH6 database (Lynch and Truhlar 2003), GGA functionals systematically underestimate the barriers, with a MUE between 7.8 and 9.4 kcal/mol. Better results were obtained with HGGA functionals, with MUE around 4.5–5.0 kcal/mol. The mPWPW91 MGGA functional is not a clear improvement, with a MUE of 8.5 kcal/mol, while HMGGA functionals such as the mPW1PW91 and the MPW1K perform better, with MUE of 3.9 and 1.4 kcal/mol, respectively (Zhao et al. 2004). Testing the functional on the larger BH42/04 database, consisting of 42 transition-state barrier heights of hydrogen transfer reactions in mostly open-shell systems, gave substantially similar results (Zhao & Truhlar 2004). The HGGA functionals underestimate barriers by a MUE of roughly 4 kcal/mol, while HMGGA functionals give better results, with peak performances from the BB1K, XB1K, and MPWB1K resulting in MUE around 1.2–1.3 kcal/mol. Similar conclusions are achieved when the HTBH38 database, which contains 38 transition-state barrier heights for 19 hydrogen transfer reactions, 18 of which involve radicals as reactant and product, is considered. In this case, 10 examined HGGA functionals result in an average MUE of 3.7 kcal/mol, while 7 range-corrected functionals slightly decrease this value to 2.7 kcal/mol (Peverati and Truhlar 2014). Moving to 38 transition-state barrier heights for non-hydrogen transfer reactions constituting the NHTBH38/04 database, and comprising 12 barrier heights for heavy-atom transfer reactions, 16 barrier heights for nucleophilic substitution reactions, and 10 barrier heights for non nucleophilic substitution unimolecular and association reactions, GGA functionals, such as the PBE, still approximate barriers severely, with a MUE of 8.64 kcal/mol. HGGA functionals, such as the B3LYP and the PBE1PBE functionals, perform better, although the MUE, around 4 kcal/mol, still is quite large (Zhao et al. 2005). MGGA functionals perform similarly to the GGA functionals, while the performance of HMGGA is rather scattered. For example, the TPSSh and the MPW1KCIS functionals do not perform impressively, with MUE of 6.6 and

Table 8 Selected mean errors for HTBH38 and NHTBH38 database

Method		Hydrogen transfer	Heavy atom transfer	Nucleophilic substitution	Unimolecular and association
PBE	GGA	9.32	14.93	6.97	3.35
BLYP	GGA	7.52	14.66	8.40	3.51
B3LYP	HGGA	4.23	8.49	3.25	2.02
PBE1PBE	HGGA	4.22	6.62	2.05	2.16
TPSS	MGGA	7.71	14.65	7.75	4.04
TPSSKCIS	MGGA	4.69	9.26	4.88	2.12
TPSSh	HMGGA	5.97	11.51	5.78	3.23
BB1K	HMGGA	1.16	1.58	1.30	1.44

4.6 kcal/mol, respectively, while the MPW1K and the BB1K are very accurate, with MUE of 1.3 and 1.2 kcal/mol, respectively (Zhao and Truhlar 2005a). As for hydrogen transfer reactions, comparison between 7 range-separated functionals and 10 HGGA functionals indicated that the range-separated functionals, with an average MUE of 2.9 kcal/mol, perform slightly better than the HGGA functional, with an average MUE of 3.7 kcal/mol. However, the peak performance of the MPW1K and B97-3 HGGA functionals, with MUE around 1.5 kcal/mol, is not reached by any of the range-separated functionals, with a minimum MUE of 2.41 kcal/mol achieved by the ωB97 functional (Peverati and Truhlar 2014).

The breakdown of these cumulative MUEs for selected functionals is reported in Table 8. Clearly, the most problematic cases are the transfer reaction of both hydrogen and heavy atoms. With the exception of the BB1K, all the other functionals fail to a large and embarrassing extent. For the HTBH38 dataset, the M06 and M06-2X HMGGA functionals, with MUE of 2.00 and 1.13 kcal/mol, also perform well (Zhao and Truhlar 2005a). Barrier heights of nucleophilic substitutions are predicted better, although GGA functionals still result in a too large MUE. Finally, the barrier heights of unimolecular and association reactions are predicted with reasonably accuracy by all functionals. Again, the performance of the BB1K functional is extremely good for the four classes of reactions considered. Similarly good and well-balanced performances are also obtained with other HMGGA functionals such as the PW6BK and the MPWB1K functionals.

Similar extensive tests on another dataset, comprising the barrier height for 23 reactions of small systems with a radical transition state, also highlighted the good performances of the HMGGA BB1K functional, with a MUE of 1.05 kcal/mol, in predicting energy barriers. However, when the same functionals were tested on a dataset of 6 barrier heights of larger systems with a singlet transition state, the best performance was obtained with the simple HGGA B1LYP functional, with a MUE of 2.58 kcal/mol, and the performance of the B3LYP functional, with a MUE of 3.10 kcal/mol, was slightly worse, while all the HMGGA functionals tested, including the BB1K functional, resulted in MUE greater than 4 kcal/mol (Riley et al. 2007).

Table 9 First metal–carbonyl dissociation energy, in kcal/mol, for selected first-row transition metal systems. DFT values, calculated with the TZVP basis set on the metal, and the SVP or TZVP basis sets on CO

		$Ni(CO)_4$		$Fe(CO)_5$		$Cr(CO)_6$	
Exp.		24.9 ± 2^a		41.5 ± 2^b		36.8 ± 2^b	
Method		SVP	TZVP	SVP	TZVP	SVP	TZVP
BP86	GGA	32.3	29.4	50.1	46.8	46.0	42.8
PW91	GGA	34.3	31.4	52.8	49.4	48.6	45.5
revPBE	GGA	33.9	30.9	52.1	48.6	48.2	44.9
B3LYP	HGGA	24.2	21.3	42.1	38.8	39.8	36.5
PBE1PBE	HGGA	29.2	26.4	50.1	47.1	46.1	43.4
B98	HGGA	25.6	22.8	44.7	41.8	41.5	38.6
TPSS	MGGA	32.9	30.5	50.8	48.1	46.2	43.8
mPWKCIS	MGGA	30.3	27.3	48.4	44.8	44.7	41.3
BB95	MGGA	30.4	27.4	48.8	45.2	45.4	42.4
TPSSh	HMGGA	31.2	28.6	50.0	47.4	45.5	43.0
M06	HMGGA	25.6	22.5	44.2	40.3	45.0	41.7

Eight: Bond Energies

The performance of several functionals to predict bond energies on a database of 21 metal–ligand bond energies, the MLBL21/05 database (Schultz et al. 2005a), indicated that GGA functionals predict metal–ligand bond energies with a MUE between 6 and 12 kcal/mol, with the BLYP, PBE, and BP86 among the worst, and that performances can be quite better at the HGGA level, with MUE normally in the 5–7 kcal/mol range. MGGA and HMGGA functionals do not offer an improvement, as exemplified by the MUE of the TPSS and TPSSh functionals, 7.9 and 5.5 kcal/mol, respectively, and by the M06 functional, with a MUE of 5.4 kcal/mol (Zhao and Truhlar 2008b).

Taking again some selected binary carbonyl complexes of first-row transition metals as examples, the performance of various functionals in the prediction of the first bond dissociation energy is reported in Table 9. The first clean result is that the binding energy is strongly affected by the basis set quality, and a triple-ζ basis set yields binding energies that are roughly 3–4 kcal/mol lower. Focusing on the TZVP results, the GGA functionals examined consistently overestimate the CO binding energy in the three complexes by roughly 3–6 kcal/mol. The PBE1PBE HGGA functional performs like the GGA functionals examined, whereas the B3LYP, and particularly the B98 functional, is among the best performing functionals. Meta-functionals only offer a marginal improvement.

Nine: Hydrogen Bonding

Benchmarking various DFT methods to reproduce the H–bond interaction energy of ten systems composed by main group atoms revealed that HGGA functionals generally perform better than GGA functionals, with MUE around 0.5 kcal/mol, and the B3LYP functional among the best. GGA functionals, instead, result in

Table 10 H-bond interaction energy, in kcal/mol, of selected nucleic acid base pairs

Base pair	MP2/aug-cc-pVQZ	B3LYP/6-31G(d,p)	PW91/6-31G(d,p)
G:C Watson–Crick	−27.7	−25.5	−27.7
A:T Watson–Crick	−15.1	−12.3	−14.5
G:U Wobble	−15.7	−13.4	−14.8
U:U Calcutta	−9.6	−7.5	−8.7

MUE between 0.5 and 2.0 kcal/mol, with the BLYP, MPWPW91, and MPWPBE among the best performing (Riley et al. 2007). MGGA and HMGGA functionals perform close to the B3LYP functional. In all cases, the quality of the basis sets had a strong impact on the quality of the results, and at least a 6-31G(d,p) basis set should be used. Further tests were performed on a database consisting of the binding energies of 6 hydrogen bonding dimers, the HB6/04 database (Zhao and Truhlar 2005b). Also these tests indicated that the performance of GGA functionals is generally not very impressive, with MUE normally between 0.5 and 4 kcal/mol, with the exception of the very well-performing PBE functional, with a MUE of 0.25 kcal/mol only. On the average HGGA performs better, with MUE between 0.3 and 1.0 kcal/mol, with the PBE1PBE functional, with a MUE of 0.27 kcal/mol, among the best, while the B3LYP functional, with a MUE of 0.87 kcal/mol, does not perform impressively. Meta-GGA and meta-HGGA functionals are not a great improvement. These results have been achieved with the rather large aug-cc-pVTZ basis set, using the 6-31+G(d,p) basis set leading to slightly lower performances.

Extensive tests of the performance of the B3LYP and PW91 functionals in the case of H-bonded nucleic acid–base pairs indicated that the PW91 GGA functional replicates with better accuracy the MP2/aug-cc-pVQZ values than the B3LYP HGGA functional (Sponer et al. 2004). The B3LYP calculations underestimate the interaction energies by few kcal/mol with relative error of 2.2 kcal/mol. Representative values for Watson–Crick (G–C, A–T) purine–pyrimidine (G–U) and pyrimidine–pyrimidine (U–U) pairs are presented in Table 10.

Ten: Weak Interactions

For a long time, one of the well-known failures of DFT was in the description of long-range dispersion forces, which are the glue that keeps together Van der Waals complexes and are at the basis of the well-known $\pi - \pi$ stacking interactions. Members of the former family are the rare-gas dimers that almost invariably are predicted to be unbound (or bound by effect of the basis set superposition error) by many GGA and HGGA functionals. Indeed, an extensive benchmark on the WI4/04 datasets, composed by four rare-gas dimers (HeNe, NeNe, HeAr, and NeAr) indicated that the B3LYP functional simply does not predict a energy well for three out of the four dimers if the basis set superposition error is corrected by the counterpoise procedure and that even including the basis set superposition error the interaction energy is underestimated by 0.23 kcal/mol, and equilibrium distances are overestimated by more than 1 Å. On the other hand, HMGGA functionals were shown to reproduce with good accuracy both the interaction energy and the

equilibrium distance of these dimers, with MUE on the counterpoise-corrected binding energies below 0.05 kcal/mol by several functionals, such as the X1B95 and the MPWB1K, and with MUE on the equilibrium distances as low as 0.10 Å, which is a remarkable result for weakly interacting systems (Zhao and Truhlar 2004).

Enlarging the dataset to include also organic molecules, such as the C_6H_6–Ne, and the $(C_2H_4)_2$ and $(CH_4)_2$ dimers, indicated that standard GGA functionals systematically underestimate the interaction energy by a MUE of roughly 0.4–1.0 kcal/mol, with the exception of the PBE functional, with a MUE of 0.30 kcal/mol. MGGA functionals do not perform much better, while a small improvement is shown by HGGA functionals, with the best results from B97-1 with a MUE of 0.20 kcal/mol. HMGGA functionals do not offer better performances, although the largest MUE is reduced to 0.64 kcal/mol (Zhao and Truhlar 2005b). Finally, better performances were shown by the M05-2X and M06-2X functionals, with a MUE of only 0.03 and 0.09 kcal/mol, respectively, when applied to a dataset formed by the four rare-gas dimers above, $C_6H_6 - Ne$, $CH_4 - Ne$, and the $(CH_4)_2$ dimer. Surprisingly, on this reduced dataset, the well-performing B97-1 functional was not tested (Zhao and Truhlar 2005b).

Moving to $\pi - \pi$ stacking interactions, the performance of a series of functionals was tested on the PPS5/05 database, which consists of binding energies of five $\pi - \pi$ stacking complexes, namely, $(C_2H_2)_2$, $(C_2H_4)_2$, and sandwich, T-shaped, and parallel-displaced $(C_6H_6)_2$ (Zhao and Truhlar 2005a). Basically, all the functionals tested underestimated the binding energies in the PPS5/05 database, with MUE in the range of 1.0–3.8 kcal/mol. This is not a minor failure, since the average binding energy in the PPS5/05 dataset amounts to 2.02 kcal/mol only. The PBE GGA functional, with a MUE of 2.1 kcal/mol, performs better than the B3LYP HGGA functional, which results in a MUE of 3.2 kcal/mol. The best performances, slightly above 1 kcal/mol, are obtained with the PWB6K, PW6B95, and MPWB1K. A clear improvement is obtained with the M06-2X functional, with a MUE of 0.30 kcal/mol only. Reducing the amount of Hartree–Fock exchange deteriorates somewhat performances, as evidenced by the MUE of 0.60 kcal/mol yielded by the M06 functional Zhao and Truhlar 2008b).

Focusing on $\pi - \pi$ stacking interactions between nucleic acid bases, which are fundamental to describe properly the base–base stacking in nucleic acids, the popular B3LYP is simply unable to find a minimum corresponding to the A···T as well as the G···C base pairs in a stacked geometry. Of the six functionals tested, only the MPWB1K and the PWB6K functionals resulted in stable stacked base pairs, with an underestimation of the stacking energy of roughly 2–3 kcal/mol (Zhao & Truhlar 2005c).

Range-separated functionals, which were developed with the particular intent of describing properly the exchange term at long distances, offer a clear improvement over the performance of classic HGGA functionals on weak interacting systems. For example, when the performance of different families of functionals is compared through the NCCE31/05 database, which comprises the various databases described above, seven range-separated functionals, including the CAM-B3LYP, the LC-ωPBE, and the ωB97 functionals, with an average MUE of

0.61 kcal/mol, perform clearly better than 10 HGGA functionals, with a MUE of 0.92 kcal/mol. However, it is important to remark that on the same NCCE31/05 database, functionals fitted to reproduce non-covalent interactions, as the M06 functional, with a MUE of 0.41 kcal/mol, also perform remarkably well (Peverati and Truhlar 2014).

As a final remark, we note that, based on an idea earlier proposed for Hartree–Fock calculations (Hepburn et al. 1975; Ahlrichs et al. 1977), the addition of an empirical $C_6 \cdot R^{-6}$ dispersion term represents a very simple cure to the failure of standard density functionals to predict dispersion interactions (Grimme 2006b). This approach is treated extensively in Chapter 12, so we do not discuss it here in details. We only remark the very good performance of a range-separated functional that also include an empirical dispersion term, such as the wB97X-D functional, on the NCCE31/05 database, with a MUE of only 0.32 kcal/mol.

Eleven: Spin States

The problem of a reliable prediction of the relative ordering of different spin states in transition metal complexes remains a tough challenge for DFT – not only for a quantitative judgment (energy separation between the different spin states) but even for a qualitatively assessment (correct prediction of the spin ground state). There is general consensus that GGA functionals overestimate the stability of low-spin states, whereas the inclusion of Hartree–Fock exchange in the HGGA functionals results in an overestimation of the stability of high spin states (Ghosh 2006; Swart 2008). This led to the development of the B3LYP* functional, in which the amount of the Hartree–Fock exchange is reduced from 20 % of the original B3LYP functional to 15 % (Reiher et al. 2001). Furthermore, it has been suggested that results obtained with Slater-type basis sets converge rapidly with the basis set size, while this convergence in case of Gaussian-type basis sets is much slower, and demanding basis sets like Dunning's correlation-consistent basis are needed to achieve good results (Güell et al. 2008).

Besides the above general comment, benchmark tests of the different functionals in this case are often hampered by the problem of accurate reference data and by the problem that functionals that seem to behave properly for a metal or system simply fail if the system changes (Ghosh 2006). Focusing on Fe complexes, a benchmark study versus CASPT2 values (see Table 11) indicated that the OPBE functional performs definitely better than commonly used GGA and HGGA functionals. In a similar study, the performance of some DFT functionals to describe CASPT2 results for a series of five Fe complexes indicated that the OLYP functional performed remarkably well in these cases, whereas the success of the HGGA PBE1PBE, B3LYP, and B3LYP* functionals varied from case to case (Pierloot and Vancoillie 2008). Finally, another benchmark study, in which various properties of Fe_2, Fe_2^-, and FeO^+, as obtained from a series of GGA, HGGA, MGGA, and HMGGA functionals, were calculated, indicated that no single functional was found to yield a satisfactory description of all characteristics for all states of these species (Sorkin et al. 2008). These results clearly indicate that the spin-state problem still is an open challenge for DFT.

Table 11 Singlet–quintet splitting, $E_{singlet}$–$E_{quintet}$ in kcal/mol, for selected Fe complexes (Swart 2008)

	$Fe(H_2O)_6^{2+}$	$Fe(NH_3)_6^{2+}$	$Fe(bpy)_3^{2+}$	MAD
CASPT2	46.6	20.3	−13.2	
BP86	28.4	5.1	−23.2	14.5
RPBE	34.3	6.3	−29.9	14.3
B3LYP	33.1	14.1	0.6	11.2
PBE1PBE	46.0	24.7	9.0	9.1
OPBE	49.3	19.0	−14.9	1.9

MAD mean absolute deviation

Twelve: Excited States

Testing the performance of several functionals in the TD-DFT prediction of 21 valence and 20 Rydberg excitation energies in N_2, O_2, HCOOH, and tetracene indicated that valence excitations are easier to predict than Rydberg excitation. Indeed, valence excitations were predicted by 15 functionals with a MUE of 0.36 eV, while Rydberg excitations were predicted with a MUE of 1.13 eV. Focusing on valence excitations, HMGGA functionals such as TPSSh, B98, and B97-3 are the best performers, with MUE as small as 0.25 eV. Nevertheless, GGA and HGGA functionals, with a MUE of 0.32 and 0.28 eV for the PBE and B3LYP functionals, respectively, also perform reasonably well. Differently, for the accurate prediction of Rydberg excitations, a high amount of Hartree–Fock exchange, as in the M06-2X and M06-HF functionals, with MUE lower than 0.4 eV, is beneficial. With the exception of the also well-performing BMK functional, almost all the other functionals tested results in MUE greater than 0.78 eV, with the PBE and B3LYP functionals resulting in a MUE of 1.95 and 1.07 eV, respectively. When Rydberg and valence excitations are combined into a single database, the best average performance is of the M06-2X and BMK functionals, with a MUE around0.35 eV (Zhao and Truhlar 2008b).

With regards to charge-transfer excitations, the performance of 16 functionals was tested in the prediction of three charge-transfer excitation energies in tetracene and in the $NH_3 \cdot\cdot F_2$ and $C_2H_4 \cdot\cdot C_2F_4$ complexes. The average MUE over the 16 functionals examined, 3.86 eV, is depressive. The only working functional is M06-HF, with a MUE of 0.09 eV. However, the inclusion of Hartree–Fock exchange is not the only reason for this surprisingly good performance, since simple HF and the HFLYP functional results in MUE around 1 eV. With the exception of the M05-2X and M06-2X, with a MUE around 2.5 eV, all the other functionals tested resulted in a MUE greater than 3 eV (Zhao and Truhlar 2008b). As a final note, it would be interesting to test the performance of the M06-HF on a larger database.

Moving to more complex organic molecules, the $\pi \rightarrow \pi^*$ transitions of more than 100 dyes from the major classes of chromophores have been investigated using a TD-DFT with the PBE, PBE1PBE, and long-range corrected hybrid functionals. The PBE1PBE and CAMB3LYP were shown to outperform all other approaches, with the latter functional especially adequate to treat molecules with delocalized

excited states. The PBE1PBE functional resulted in a MUE of 22 nm (0.14 eV) with no deviation exceeding 100 nm (0.50 eV), thus delivering reasonable estimates of the color of most organic dyes of practical or industrial interest. Long-range functionals allowed a better description of the low-lying excited-state energies than HGGA functionals, and linearly corrected long-range approaches yield an average error of 10 nm (Jacquemin et al. 2008).

An extended test of the performance of 41 functionals in the calculation of the electronic absorption spectra of Cu and Zn complexes by TD-DFT methods indicated that HGGA functionals outperform GGA functionals. In the case of the spin-unrestricted calculations on the Cu^{II}(thiosemicarbazonato) complex, the functional best performing in the reproduction of the experimental spectra and geometry was the B1LYP, while the B3LYP functional was ranked 8. This order was not replicated in case of the spin-restricted Zn^{II}(thiosemicarbazonato) complex, where the best functional was PBE1PBE, with the B3LYP ranked 10. In both cases, HGGA functionals did not offer an improvement. In almost all the cases, the calculations underestimated the experimental excitation energies (Holland and Green 2010). Nevertheless, it is may be worth noting that the OPBE and the OBLYP functionals, which were shown to perform well in other cases, were not considered.

Orbitals in DFT

Since chemists long have used and continue to use orbitals as natural language to explain and rationalize the complex reality of molecules that define the realms of inorganic and organic chemistry, we conclude with a few remarks on orbitals obtained from density functional calculations.

Originally, chemists have built their understanding of orbitals on constructs that resulted from WFT analyses, and such an orbital is usually referred to as molecular orbital (MO). One important aspect of an MO analysis is the investigation of orbital overlap. A simplified wave function theory that emphasizes this particular feature of orbital interaction, the extended Hückel theory (EHT), has revolutionized the general perception of molecular structure and reaction mechanisms.

Since the Kohn–Sham orbitals, introduced and used in DFT, serve a different purpose than creating a reasonable single determinantal wave function Ψ, chemists were seeking answers to the question "what do the Kohn–Sham orbitals and eigenvalues mean?" as DFT moved into the spotlight of electronic structure theory. A simple answer was based on a comparison of orbitals of small molecules (H_2O, N_2, $PdCl_4^{2-}$) obtained from WFT (Hartree–Fock, EHT) and DFT calculations: The shape and symmetry properties of the KS orbitals are very similar to those calculated by HF and EHT methods. The energy order of the occupied orbitals is in most cases in agreement between WFT and DFT methods. Overall, the KS orbitals are a good basis for qualitative interpretation of molecular orbitals (Stowasser and Hoffmann 1999). This simple conception of the meaning and the use of KS orbitals by now has gained general acceptance, and chemists often use KS orbitals in ways that are familiar to them from MO analysis.

Baerends and Gritsenko (1997) have provided an answer to the same question based on fundamental concepts of density functional theory. Among other aspects, the authors identify the following two important characteristics of KS orbitals:

1. The highest occupied Kohn–Sham orbital energy is equal to the exact first ionization energy. This is a property that is very desirable in qualitative MO theory in general and is often simply assumed in such theories.
2. The lowest unoccupied Kohn–Sham orbital energy and all other virtual orbital energies are solutions in exactly the same potential as the occupied orbitals. They are therefore not shifted toward higher energies in the same way as Hartree–Fock virtual orbitals are – HF orbital energy differences are not estimates of excitation energies. Further, it has been observed empirically for a long time that KS orbital energy differences are good approximations to excitation energies, and the KS orbital energy differences play a role as a first approximation to the excitation energy in the treatment of excitation energies using time-dependent DFT.

The authors therefore recommend KS orbitals and one-electron energies as tools in the traditional qualitative MO considerations on which much of the rationalizations of contemporary chemistry are based. The Kohn–Sham one-electron model and KS orbitals provide an ideal MO theoretical context to apply concepts such as "charge control" and "orbital control." KS orbitals usually follow the expected behavior, in terms of bonding and antibonding character in terms of geometrical distortions and in terms of interaction with other atoms or molecules.

About 10 years later, Cramer and Truhlar (2009) presented a more conservative view of the use of KS orbitals. One should be careful not to stretch the interpretation of KS orbitals beyond its limits, since KS orbitals correspond to a fictitious noninteracting system with the same electron density as the correct many-body function. Since the density computed from KS orbitals is an approximation to the exact density, properties that depend on individual orbitals, with the exception of the energy of the highest occupied orbitals, should be interpreted with care. Nonetheless, many studies published in the literature do employ DFT molecular orbitals to interpret the electronic origins of chemical bonding and reactivity.

The quality of the KS orbitals depends to a large part on the ability of a chosen density functional to correctly represent the ground-state density of a given molecule. In most cases, different density functionals produce qualitatively identical orbitals, which also agree with WFT orbitals. For molecules that might posses a spin-polarized ground-state density, different methods of electronic structure calculation not only produce *quantitatively* different results but also lead to *qualitatively* contrastive conclusions. One such case is illustrated in Fig. 7.

Figure 7 Energies and shapes of the two highest occupied (red-blue) and the two lowest unoccupied (yellow-green) KS orbitals (contour envelope 0.05 a.u.) of $Fe(S_2C_2H_2)_2$ extracted from an unpolarized ground-state density according to GGA and HGGA DFT calculations. The molecule was constructed according to D_{2h} symmetry with a Fe–S bond length of 220 pm. Also shown for the sake of comparison are orbitals obtained from an extended Hückel calculation.

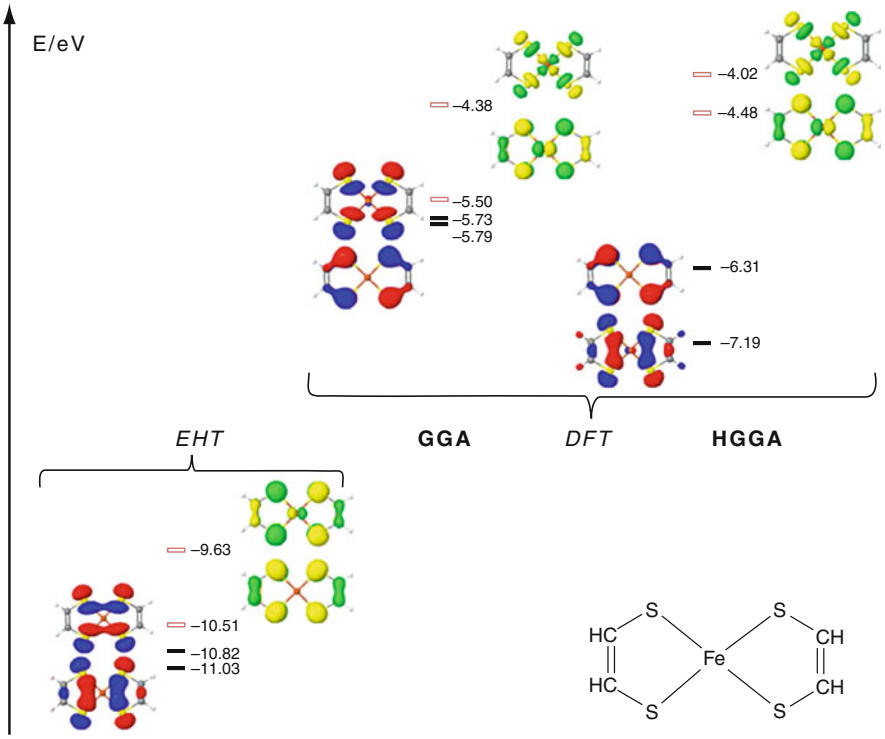

Fig. 7 Energies and shapes of the two highest occupied (*red-blue*) and the two lowest unoccupied (*yellow-green*) KS-orbitals (contour envelope: 0.05 a.u.) of $Fe(S_2C_2H_2)_2$ extracted from an unpolarized ground state density according to GGA and HGGA DFT calculations. The molecule was constructed according to D_{2h} symmetry with a Fe-S bond length of 220 pm. Also shown for the sake of comparison are orbitals obtained from an extended Hückel calculation

But the essential understanding of chemical orbitals itself is open to interpretation; Autschbach (2012) elaborates on the use and misuse of orbitals in quantum theory and chemistry. Naturally, KS orbitals play an essential role in this challenging controversy. We leave it to the reader to decide whether or not chemically meaningful information can be extracted from the orbital picture as displayed in Fig. 7.

DFTips

The advertent reader has noticed the many technical recommendations that we have given within the discussion of the twelve selected scenarios for properties of atoms and molecules. Here, we will close our instruction manual with a few pieces of general advice.

B3LYP Is No Synonym for DFT

Some researchers hold the opinion that given the fact that the B3LYP functional has been identified as the most successful DFT method in an overwhelming number of systematic investigations in very many areas of chemical research, there is no persuasive motivation to recommend its replacement by one of the other functionals. We do not agree with such a judgment. Although the B3LYP functional is largely responsible for DFT becoming one of the most popular tools in computational chemistry, it does have unsatisfactory performance issues, notably the unreliable results obtained for transition metal chemistry (Zhao and Truhlar 2008a). One should become aware of the capabilities and shortcomings of particular density functionals. It might well be that B3LYP is the proper approach to many chemical problems, but choosing a functional for its previous success while ignoring its potential failures cannot be the right strategy to approach DFT calculations.

Choose Your DFT Method Carefully

We agree with Burke's interpretation of "The good, the bad and the ugly": It is *good* to choose one functional of each kind and stick with it. It is *bad* to run several functionals and pick the "best" answer. And it is *ugly* to design your own functional with 2300 parameters.

In view of the many functionals available, it is likely that one will find a functional that fits one's own particular problems. In view of possibilities offered by computational programs that make it fairly easy to create new sets of parameterized hybrid functionals, it is almost certain that for each chemical problem, the right functional can be designed.

Following such an approach, density functional calculations lose their generality and meaning. One should aim for consistency within one's calculations, rather than for the best agreement with experiment. If one choose a particular functional for its characteristics and capabilities, the results of DFT calculations gain a predictive quality.

Read the Fine Print

During the early days of HGGA development, it became clear that B3LYP is not B3LYP (Hertwig and Koch 1997). Different programs based their implementation of the B3LYP functional on different models of the underlying LDA and produced slightly different results for the same chemical problem. The same considerations apply to the gradient corrections for correlation; P86 requires a different choice of LDA than LYP. Some computer programs automatically make the right choice, while other programs rely on correct input instructions given by the user.

Familiarize yourself with the default values and basic implementations of your favorite DFT code. Default values are chosen with much consideration and, most of the time, are just adequate. However, for subtle problems, you might find it necessary, for example, to change the accuracy of the numerical integration routines.

DFT Does Not Hold the Universal Answer to All Chemical Problems

You can expect that not all of your DFT calculations will produce satisfying results. An increasing number of problem molecules are currently identified for which standard density functionals fail to produce satisfactory results. Seemingly simple stereoelectronic effects in alkane isomers provided a serious challenge for many standard functionals, such as B3LYP, BLYP, or PBE (Grimme 2006c). However, such failures are not bad news for DFT but rather good news. The origin of the dissatisfying DFT performance has been carefully analyzed and led to the design of improved functionals (Zhao et al. 2006). Be honest with your DFT results and accept apparent failures – it might be just another small step climbing Jacob's ladder.

Make DFT an Integral Part of Your Work

Although in some areas of chemical research DFT is at the verge of becoming a standard research tool, necessary for the complete characterization of new molecules, not every chemical problem warrants a full-fledged DFT investigation. However, if you structure your computational approach beginning with an elaboration of qualitative aspects before addressing a problem in a quantitative way, a few quick DFT calculations might provide you with valuable insights how to further pursue your line of work.

Follow Your Interests

As final advice we will leave you with the words of Nobel Prize laureate Harold Kroto: Do something which interests you or which you enjoy, and do it to the absolute best of your ability. If it interests you, however mundane it might seem on the surface, still explore it because something unexpected often turns up just when you least expect it.

We hope that our work could satisfy some old interests as well as perk some new interests. We wish that our short instruction manual serves as a valuable guide for the perplexed and provides some food for thought for the enlightened, be it in agreement or in disagreement. If you follow your interests, keep an open mind, and maintain a broad perspective, good things will happen.

Bibliography

The literature on DFT is large and rich in excellent reviews and overviews. At the same time, while thousands of papers on DFT have been published, most of them will become out of date in the future, as the picture and perception of DFT, chemistry, and science in general is in a state of constant flux. It was necessary to make a conscious selection that of course is not unbiased – some references represent the most recent developments in DFT, while others have been part of our DFT folder for a long time. The reader will find references to books, review articles, and articles that illustrate developments and applications of DFT.

Books on DFT

Fiolhais, C., Nogueira, F., & Marques, M. (Eds.). (2003). *A primer in density functional theory (lecture notes in physics)*. Berlin/New York: Springer.

Koch, W., & Holzhausen, M. C. (2002). *A chemist's guide to density functional theory* (2nd ed.). Weinheim/New York: Wiley.

Marques, M. A. L., Ullrich, C. A., Nogueira, F., Rubio, A., Burke, K., & Gross, E. K. U. (Eds.). (2006). *Time-dependent density functional theory (lecture notes in physics)*. Berlin: Springer.

Parr, R. G., & Yang, W. (1989). *Density functional theory of atoms and molecules*. New York: Oxford University Press.

Reviews and Overviews of DFT

Baerends, E. J., & Gritsenko, O. V. (1997). A quantum chemical view of density functional theory. *Journal of Physical Chemistry A, 101*, 5383–5403.

Becke, A. D. (2014). Perspective: Fifty years of density-functional theory in chemical physics. *Journal of Chemical Physics, 140*, art. 18A301.

Cohen, A. J., Mori-Sánchez, P., & Yang, W. (2012). Challenges for density functional theory. *Chemical Reviews, 112*, 289–320.

Cramer, C. J., & Truhlar, D. G. (2009). Density functional theory for transition metals and transition metal chemistry. *Physical Chemistry Chemical Physics, 11*, 10757–10816.

Geerlings, P., De Proft, F., & Langenaeker, W. (2003). Conceptual density functional theory. *Chemical Reviews, 103*, 1793–1873.

Kohn, W., Becke, A. D., & Parr, R. G. (1996). Density functional theory of electronic structure. *Journal of Physical Chemistry, 100*, 12974–12980.

Neese, F. (2009). Prediction of molecular properties and molecular spectroscopy with density functional theory: From fundamental theory to exchange-coupling. *Coordination Chemistry Reviews, 253*, 526–563.

Perdew, J. P., Ruzsinszky, A., Constantin, L. A., Sun, J. W., & Csonka, G. I. (2009). Some fundamental issues in ground-state density functional theory: A guide for the perplexed. *Journal of Chemical Theory and Computation, 5*, 902–908.

Sousa, S. F., Fernandes, P. A., & Ramos, M. J. (2007). General performance of density functionals. *Journal of Physical Chemistry A, 111*, 10439–10452.

Ziegler, T. (1991). Approximate density functional theory as practical tool in molecular energetics and dynamics. *Chemical Reviews, 91*, 651–667.

Ziegler, T. (1995). Density functional theory as practical tool in studies of organometallic energetics and kinetics. Beating the heavy metal blues with DFT. *Canadian Journal of Chemistry, 73*, 743–761.

Zhao, Y., & Truhlar, D. G. (2008a). Density functionals with broad applicability in chemistry. *Accounts of Chemical Research, 41*, 157–167.

Conceptual Developments and Applications of DFT

Ahlrichs, R., Penco, R., & Scoles, G. (1977). Intermolecular forces in simple systems. *Chemical Physics, 19*, 119–130.

Baerends, E. J., Ellis, D. E., & Ros, P. (1973). Self-consistent molecular Hartree-Fock-Slater calculations – I. The computational procedure. *Chemical Physics, 2*, 41–47.

Baerends, E. J., & Ros, P. (1978). Evaluation of the LCAO Hartree-Fock-Slater method – Applications to transition-metal complexes. *International Journal of Quantum Chemistry, 12*, 169–190.

Bartlett, R. J., Lotrich,V. F., & Schweigert, I. V. (2005). Ab initio density functional theory: The best of both worlds? *Journal of Chemical Physics, 123*, art. 062205.

Becke, A. D. (1988a). Density-functional exchange-energy Approximation with correct asymptotic behavior. *Physical Review A, 38*, 3098–3100.

Becke, A. D. (1988b). A multicenter numerical-integration scheme for polyatomic molecules. *Journal of Chemical Physics, 88*, 2547–2553.

Becke, A. D., & Roussel, M. R. (1989). Exchange holes in inhomogeneous systems – A coordinate-space model. *Physical Review A, 39*, 3761–3767.

Becke, A. D. (1993a). A new mixing of Hartree-Fock and local density-functional theories. *Journal of Chemical Physics, 98*, 1372–1377.

Becke, A. D. (1993b). Density-functional thermochemistry: 3. The role of exact exchange. *Journal of Chemical Physics, 98*, 5648–5652.

Boerrigter, P. M., te Velde, G., & Baerends, E. J. (1988). 3-dimensional numerical-integration for electronic-structure calculations. *International Journal of Quantum Chemistry, 33*, 87–113.

Furche, F. (2008). Developing the random phase approximation into a practical post-Kohn–Sham correlation model. *Journal of Chemical Physics*, *129*, art. 114105.

Gill, P. M. W. (2001). Obituary: Density functional theory (1927–1993). *Australian Journal of Chemistry, 54*, 661–662.

Grimme, S. (2006*a*). Semiempirical hybrid density functional with perturbative second-order correlation. *Journal of Chemical Physics*, *124*, art. 034108.

Hepburn, J., Scoles, G., & Penco, R. (1975). Simple but reliable method for prediction of intermolecular potentials. *Chemical Physics Letters, 36*, 451–456.

Hertwig, R. H., & Koch, W. (1997). On the parameterization of the local correlation functional. What is Becke-3-LYP? *Chemical Physics Letters, 268*, 345–351.

Hohenberg, P., & Kohn, W. (1964). Inhomogeneous electron gas. *Physics Reviews, 136*, B646–B871.

Kohn, W., & Sham, L. J. (1965). Self-consistent equations including exchange and correlation effects. *Physics Reviews, 140*, A1133–A1138.

Kurth, S., & Perdew, J. P. (2000). Role of the exchange-correlation energy: Nature's glue. *International Journal of Quantum Chemistry, 77*, 814–818.

Leininger, T., Stoll, H., Werner, H. J., & Savin, A. (1997). Combining long-range configuration interaction with short-range density functionals. *Chemical Physics Letters, 275*, 151–160.

Perdew, J. P. (1986). Density-functional approximation for the correlation-energy of the inhomogeneous electron gas. *Physical Review B, 33*, 8822–8824.

Perdew, J. P., Burke, K., & Ernzerhof, M. (1996). Generalized gradient approximation made simple. *Physical Review Letters, 77*, 3865–3868.

Perdew, J. P., & Schmidt, K. (2001). Jacob's ladder of density functional approximations for the exchange-correlation energy. *Density Functional Theory and Its Applications to Materials, 577*, 1–20.

Peverati, R., & Truhlar, D. G. (2014). The quest for a universal density functional: The accuracy of density functionals across a broad spectrum of databases in chemistry and physics. *Philosophical Transactions of the Royal Society A*, *372*, art. 20120476.

Slater, J. C. (1951). A simplification of the Hartree-Fock method. *Physics Reviews, 81*, 385–390.

Tao, J. M., Perdew, J. P., Staroverov, V. N., & Scuseria, G. E. (2003). Climbing the density functional ladder: Nonempirical meta-generalized gradient approximation designed for molecules and solids, *Physical Review Letters*, *91*, art. 146401.

Tsuneda, T., & Hirao, K. (2014). Long-range correction for density functional theory. *WIREs Computational Molecular Science, 4*, 375–390.

Versluis, L., & Ziegler, T. (1988). The determination of molecular structures by density functional theory: The evaluation of analytical energy gradients by numerical integration. *Journal of Chemical Physics, 88*, 322–328.

Vosko, S. H., Wilk, L., & Nusair, M. (1980). Accurate spin-dependent electron liquid correlation energies for local spin density calculations: a critical analysis. *Canadian Journal of Physics, 58*, 1200–1211.

Zope, R. R., & Dunlap, B. I. (2006). The limitations of Slater's element-dependent exchange functional from analytic density-functional theory, *Journal of Chemical Physics*, *124*, art. 044107.

Practical Developments and Applications of DFT

Autschbach, J. (2012). Orbitals: Some fiction and some facts. *Journal of Chemical Education, 89*, 1032–1040.

Barden, C. J., Rienstra-Kiracofe, J. C., & Schaefer, H. F. (2000). Homonuclear 3d transition-metal diatomics: A systematic density functional theory study. *Journal of Chemical Physics, 113*, 690–700.

Curtiss, L. A., Raghavachari, K., Redfern, P. C., & Pople, J. A. (1997). Assessment of Gaussian-2 and density functional theories for the computation of enthalpies of formation. *Journal of Chemical Physics, 106*, 1063–1079.

Curtiss, L. A., Raghavachari, K., Redfern, P. C., & Pople, J. A. (2000). Assessment of Gaussian-3 and density functional theories for a larger experimental test set. *Journal of Chemical Physics, 112*, 7374–7383.

Ghosh, A. (2006). Transition metal spin state energetics and noninnocent systems: Challenges for DFT in the bioinorganic arena. *Journal of Biological Inorganic Chemistry, 11*, 712–714.

Grimme, S. (2006b). Semiempirical GGA-type density functional constructed with a long-range dispersion correction. *Journal of Computational Chemistry, 27*, 1787–1799.

Grimme, S. (2006c). Seemingly simple stereoelectronic effects in alkane isomers and the implications for Kohn-Sham density functional theory. *Angewandte Chemie International Edition, 45*, 4460–4464.

Güell, M., Luis, J. M., Solà, M., & Swart, M. (2008). Importance of the basis set for the spin-state energetics of iron complexes. *Journal of Physical Chemistry A, 112*, 6384–6391.

Holland, J. P., & Green, J. C. (2010). Evaluation of exchange-correlation functionals for time-dependent density functional theory calculations on metal complexes. *Journal of Computational Chemistry, 31*, 1008–1014.

Jacquemin, D., Perpete, E. A., Scuseria, G. E., Ciofini, I., & Adamo, C. (2008). TD-DFT performance for the visible absorption spectra of organic dyes: Conventional versus long-range hybrids. *Journal of Chemical Theory and Computation, 4*, 123–135.

Kelly, R. A., Clavier, H., Giudice, S., Scott, N. M., Stevens, E. D., Bordner, J., Samardjiev, I., Hoff, C. D., Cavallo, L., & Nolan, S. P. (2008). Determination of N-heterocyclic carbene (NHC)

steric and electronic parameters using the [(NHC)Ir(CO)(2)Cl] system. *Organometallics, 27*, 202–210.

Korth, M., & Grimme, S. (2009). "Mindless" DFT Benchmarking. *Journal of Chemical Theory and Computation, 5*, 993–1003.

Lynch, B. J., & Truhlar, D. G. (2003). Small representative benchmarks for thermochemical calculations. *Journal of Physical Chemistry A, 107*, 8996–8999.

Pierloot, K,. & Vancoillie, S. J. (2008). Relative energy of the high-(T-5(2g)) and low-((1)A(1g)) spin states of the ferrous complexes [Fe(L)(NHS4)]: CASPT2 versus density functional theory. *Journal of Chemical Physics*, *128*, art. 034104.

Reiher, M., Salomon, O., & Hess, B. A. (2001). Reparameterization of hybrid functionals based on energy differences of states of different multiplicity. *Theoretical Chemistry Accounts, 107*, 48–55.

Riley, K. E., Op't Holt, B. T., & Merz, K. M. (2007). Critical assessment of the performance of density functional methods for several atomic and molecular properties. *Journal of Chemical Theory and Computation, 3*, 407–433.

Schultz, N. E., Zhao, Y., & Truhlar, D. G. (2005a). Density functionals for inorganometallic and organometallic chemistry. *Journal of Physical Chemistry A, 109*, 11127–11143.

Schultz, N. E., Zhao, Y., & Truhlar, D. G. (2005b). Databases for transition element bonding: Metal-metal bond energies and bond lengths and their use to test hybrid, hybrid meta, and meta density functionals and generalized gradient approximations. *Journal of Physical Chemistry A, 109*, 4388–4403.

Sorkin, A., Iron, M. A., & Truhlar, D. G. (2008). Density functional theory in transition-metal chemistry: Relative energies of low-lying states of iron compounds and the effect of spatial symmetry breaking. *Journal of Chemical Theory and Computation, 4*, 307–315.

Sponer, J., Jurecka, P., & Hobza, P. (2004). Accurate interaction energies of hydrogen-bonded nucleic acid base pairs. *Journal of the American Chemical Society, 126*, 10142–10151.

Stowasser, R., & Hoffmann, R. (1999). What do the Kohn-Sham orbitals and eigenvalues mean? *Journal of the American Chemical Society, 121*, 3414–3420.

Swart, M. (2008). Accurate spin-state energies for iron complexes. *Journal of Chemical Theory and Computation, 4*, 2057–2066.

Wang, N. X., & Wilson, A. K. (2004). The behavior of density functionals with respect to basis set. I. The correlation consistent basis sets. *Journal of Chemical Physics, 121*, 7632–7646.

Wodrich, M. D., Corminboeuf, C., & Schleyer, P. v. R. (2006). Systematic errors in computed alkane energies using B3LYP and other popular DFT functionals. *Organic Letters, 8*, 3631–3634.

Yang, W. (1991). Direct calculation of electron density in density functional theory. *Physical Review Letters, 66*, 1438–1441.

Zhao, Y., Pu, J., Lynch, B. J., & Truhlar, D. G. (2004). Tests of second-generation and third-generation density functionals for thermochemical kinetics. *Physical Chemistry Chemical Physics, 6*, 673–676.

Zhao, Y., & Truhlar, D. G. (2004). Hybrid meta density functional theory methods for thermochemistry, thermochemical kinetics, and noncovalent interactions: The MPW1B95 and MPWB1K models and comparative assessments for hydrogen bonding and van der Waals interactions *J. Journal of Physical Chemistry A, 108*, 6908–6918.

Zhao, Y., & Truhlar, D. G. (2005a). Design of density functionals that are broadly accurate for thermochemistry, thermochemical kinetics, and nonbonded interactions. *Journal of Physical Chemistry A, 109*, 5656–5667.

Zhao, Y., & Truhlar, D. G. (2005b). Benchmark databases for nonbonded interactions and their use to test density functional theory. *Journal of Chemical Theory and Computation, 1*, 415–432.

Zhao, Y., Gonzalez-Garcia, N., & Truhlar, D. G. (2005). Benchmark database of barrier heights for heavy atom transfer, nucleophilic substitution, association, and unimolecular reactions and its use to test theoretical methods. *Journal of Physical Chemistry A, 109*, 2012–2018.

Zhao, Y., & Truhlar, D. G. (2005c). How well can new-generation density functional methods describe stacking interactions in biological systems? *Physical Chemistry Chemical Physics, 7*, 2701–2705.

Zhao, Y., Schultz, N. E., & Truhlar, D. G. (2006). Design of density functionals by combining the method of constraint satisfaction with parametrization for thermochemistry, thermochemical kinetics, and noncovalent interactions. *Journal of Chemical Theory and Computation, 2*, 364–382.

Zhao, Y., & Truhlar, D. G. (2008b). The M06 suite of density functionals for main group thermochemistry, thermochemical kinetics, noncovalent interactions, excited states, and transition elements: two new functionals and systematic testing of four M06-class functionals and 12 other functionals. *Theoretical Chemistry Accounts, 120*, 215–241.

Zhou, M., Andrews, L., & Bauschlicher, C. W. (2001). Spectroscopic and theoretical investigations of vibrational frequencies in binary unsaturated transition-metal carbonyl cations, neutrals, and anions. *Chemical Reviews, 101*, 1931–1961.